



An approach to constructing a homogeneous time series of soil moisture using SMOS

D. Leroux, Y.H. Kerr, E. F. Wood, A.K. Sahoo, R. Bindlish, T.J. Jackson

► **To cite this version:**

D. Leroux, Y.H. Kerr, E. F. Wood, A.K. Sahoo, R. Bindlish, et al.. An approach to constructing a homogeneous time series of soil moisture using SMOS. IEEE Transactions on Geoscience and Remote Sensing, Institute of Electrical and Electronics Engineers, 2013, 99, pp.1-13. <10.1109/TGRS.2013.2240691>. <ird-00828699>

HAL Id: ird-00828699

<http://hal.ird.fr/ird-00828699>

Submitted on 31 May 2013

HAL is a multi-disciplinary open access archive for the deposit and dissemination of scientific research documents, whether they are published or not. The documents may come from teaching and research institutions in France or abroad, or from public or private research centers.

L'archive ouverte pluridisciplinaire **HAL**, est destinée au dépôt et à la diffusion de documents scientifiques de niveau recherche, publiés ou non, émanant des établissements d'enseignement et de recherche français ou étrangers, des laboratoires publics ou privés.

1 An Approach to Constructing a Homogeneous Time 2 Series of Soil Moisture Using SMOS

3 Delphine J. Leroux, Yann H. Kerr, *Fellow, IEEE*, Eric F. Wood, Alok K. Sahoo,
4 Rajat Bindlish, *Senior Member, IEEE*, and Thomas J. Jackson, *Fellow, IEEE*

5 **Abstract**—Overlapping soil moisture time series derived
6 from two satellite microwave radiometers (the Soil Moisture
7 and Ocean Salinity and the Advanced Microwave Scanning
8 Radiometer-Earth Observing System) are used to generate a soil
9 moisture time series from 2003 to 2010. Two statistical methodolo-
10 gies for generating long homogeneous time series of soil moisture
11 are considered. Generated soil moisture time series using only
12 morning satellite overpasses are compared to ground measure-
13 ments from four watersheds in the U.S.A. with different clima-
14 tologies. The two methods, cumulative density function (CDF)
15 matching and copulas, are based on the same statistical theory, but
16 the first makes the assumption that the two data sets are ordered
17 the same way, which is not needed by the second. Both methods
18 are calibrated in 2010, and the calibrated parameters are applied
19 to the soil moisture data from 2003 to 2009. Results from these
20 two methods compare well with ground measurements. However,
21 CDF matching improves the correlation, whereas copulas improve
22 the root-mean-square error.

23 **Index Terms**—Advanced Microwave Scanning Radiometer-
24 Earth Observing System (AMSR-E), cumulative density func-
25 tion (CDF) matching, copulas, Soil Moisture and Ocean Salinity
26 (SMOS), soil moisture, time series.

27 I. INTRODUCTION

28 **S**OIL moisture is an important variable and is now consid-
29 ered as an essential climate variable by the World Meteorological
30 Organization [1]. It has a crucial role in the transfers
31 of water and energy between the soil and the atmosphere. Soil
32 moisture is also an input variable for land surface modeling
33 in determining the evaporative fraction at the surface and the
34 infiltration in the root zone. For both agriculture and water
35 resource management, soil moisture information is essential at
36 local and regional scales. At global scales, soil moisture is of

great value for weather forecasting [2], climate change [3], and
37 monitoring extreme events such as floods and droughts. 38

Soil Moisture and Ocean Salinity (SMOS) [4] was success-
39 fully launched by the European Space Agency in November 40
2009 and since has been providing global maps of soil moisture 41
every three days at a nominal spatial resolution of 43 km 42
with an accuracy of $0.04 \text{ m}^3/\text{m}^3$. SMOS is the first mission 43
specifically designed for soil moisture monitoring. The Soil 44
Moisture Active Passive (SMAP) mission [5] is scheduled 45
for launch in October 2014 by the National Aeronautics and 46
Space Administration. SMAP will continue the time series of 47
soil moisture based on 1.4-GHz radiometer observations that 48
began with SMOS. The 1.4-GHz frequency channel is the most 49
suitable frequency for soil moisture retrieval [6]. 50

Longer time series of satellite-based soil moisture would be 51
of value in climate-related analysis. Utilizing the data from the 52
previous generations of satellite sensors involves resolving nu- 53
merous issues. Some of the platforms and approaches have been 54
developed to retrieve soil moisture using the higher frequencies, 55
which has been the only option until now. These include the 56
Scanning Multichannel Microwave Radiometer (1978–1987) 57
[7], the Special Sensor Microwave/Imager (1987–current) 58
[7], the Advanced Microwave Scanning Radiometer-Earth 59
Observing System (AMSR-E) (2002–2011) [7], [8], Wind- 60
Sat (2003–current) [9], and the European Remote Sensing- 61
Advanced Scatterometer (1991–current) [10]. Although their 62
lowest frequencies (5–20 GHz) are not the most suitable for 63
soil moisture retrievals (higher sensitivity to vegetation growth 64
and atmospheric conditions), they remain a valuable time series 65
from 1978 until now. Applications such as data assimilation 66
or climate change assessment require consistent products. The 67
products referenced earlier have been retrieved using different 68
sensors with different algorithms, and as a result, the time series 69
is not homogeneous. This heterogeneity can be interpreted as a 70
bias and is a problem in the data assimilation process. To avoid 71
this issue, these products need to be processed to correct for any 72
bias or amplitude variation between the data sets. 73

Many previous studies have developed various methods for 74
the homogenization of time series. Vincent *et al.* [11] developed 75
a method to harmonize temperature time series with gaps. The 76
first step was to determine if the series was homogeneous by 77
comparing its anomalies to those of a reference series. The 78
identification of the gaps and their magnitude was performed 79
by successively fitting a linear model with different magnitude 80
values with the best fit being indicated by the minimum sum 81
of square errors. Homogeneous temperature and precipitation 82
time series were developed by Begert *et al.* [12] using statistical 83

Manuscript received November 28, 2011; revised May 14, 2012 and
October 22, 2012; accepted December 22, 2012. This work was supported in
part by Telespazio France and in part by TOSCA.

D. J. Leroux is with the Centre d'Etudes Spatiales de la Biosphere, 31400
Toulouse, France, and also with Telespazio France, 31023 Toulouse Cedex 1,
France (e-mail: delphine.j.leroux@gmail.com).

Y. H. Kerr is with the Centre d'Etudes Spatiales de la Biosphere, 31400
Toulouse, France (e-mail: yann.kerr@cesbio.cnes.fr).

E. F. Wood and A. K. Sahoo are with the Department of Civil and Environ-
mental Engineering, Princeton University, Princeton, NJ 08544 USA (e-mail:
efwood@princeton.edu; aksahoo2004@gmail.com).

R. Bindlish and T. J. Jackson are with the USDA ARS Hydrology and Re-
mote Sensing Laboratory, Beltsville, MD 20705 USA (e-mail: rajat.bindlish@
ars.usda.gov; tom.jackson@ars.usda.gov).

Color versions of one or more of the figures in this paper are available online
at <http://ieeexplore.ieee.org>.

Digital Object Identifier 10.1109/TGRS.2013.2240691

84 methods to detect potential inhomogeneity. In that study, a
 85 reference time series was necessary in order to detect and
 86 compute the magnitude of the shifts. Picard and Fily [13]
 87 proposed a method to simulate a homogeneous time series of
 88 the cumulative melting surface in Antarctica. Using satellite
 89 observations from different sensors and acquisition times was
 90 the biggest challenge. Correcting for the effect of the observing
 91 time was accomplished in two steps. First, a sinusoidal function
 92 with a 24-h periodicity was fitted, and then, an optimal interpo-
 93 lation to refine this first guess model to *force* it to be closer was
 94 applied to the observations and to provide very low uncertainty
 95 around observation time and larger uncertainty when there is no
 96 available observation.

97 Matching the cumulative density functions (CDFs) of two
 98 data sets has been used in several studies to merge time series.
 99 Reichle and Koster [14] and Choi and Jacobs [15] merged
 100 soil moisture derived from satellite observations with model
 101 data, and Li *et al.* [16] corrected the bias of precipitation
 102 and temperature products derived from different models. CDF
 103 matching was also used as a preliminary step of the assimilation
 104 process [17] and to produce long time series of soil moisture
 105 [18], [19].

106 Over the last few years, a new method based on copula
 107 functions has been developed. It allows the derivation of bi-
 108 variate distributions without making the assumptions required
 109 when dealing with multivariate frequency distributions, e.g.,
 110 the same type of marginal distribution for both variables, a
 111 joint normal distribution, and independent variables. One of
 112 the major advantages of the copula method is that the marginal
 113 distributions can be of any form [20]. The first comprehensive
 114 treatment of copulas was by Nelsen [21]. He presented methods
 115 to construct copulas and discussed the role played by copulas
 116 in modeling and dependence. Since then, copulas have been
 117 applied in various applications with the majority of the liter-
 118 ature dedicated to the financial sector [22], [23]. In the field of
 119 hydrology, some applications have emerged. Genest and Favre
 120 [24] summarized the existing methods to detect and evaluate
 121 the dependence between the data sets through copulas (analyt-
 122 ically and graphically) and enumerated the various methods to
 123 choose the best copula family and estimate their parameters.
 124 Favre *et al.* [25] applied copulas to peak flows and volumes
 125 from two watersheds, Salvadori and De Michele [26] to storm
 126 and rainfall time series, Dupuis [27] to the volume and duration
 127 of low flows of two rivers, Zhang and Singh [28] to rainfall fre-
 128 quency, Serinaldi and Grimaldi [29] to flood and sea frequency,
 129 and Laux *et al.* [30] to precipitation data. Gao *et al.* [31] used
 130 copulas as a preprocessing step for the assimilation process on
 131 soil moisture data.

132 Joint statistical analysis has already been applied when the
 133 sources of the soil moisture measurements come from different
 134 observation systems (e.g., AMSR-E surface soil moisture and
 135 10-cm soil moisture from a land surface model [14]). Similarly,
 136 joint statistical methods form the basis for data assimilation of
 137 satellite soil moisture into land surface models [31]. There are
 138 many other studies related to joint probability, including where
 139 the variables are physically different but where their statistical
 140 relationships are useful (e.g., rainfall storm intensity and storm
 141 duration [32]).

The goal of this paper is to estimate for all the AMSR-E 142
 period (2003–2010) SMOS-equivalent observations that can be 143
 used to develop a statistical representation of SMOS retrieval so 144
 that current and future SMOS retrievals can be used in applica- 145
 tions like drought monitoring based on percentiles. However, 146
 matching 130 am C-/X-band (AMSR-E) observations with 147
 600 am L-band (SMOS) observations presents some issues: 148
 1) The crossing times are different, and rainfalls may occur be- 149
 tween the two acquisitions; and 2) the frequencies are different, 150
 so the sensing depths are not similar. 151

The statistical impact of the rainfalls that could occur be- 152
 tween 130 am and 600 am is to lower the correlation. However, 153
 if the correlation is sufficiently high, a statistical relationship 154
 can be established to estimate an equivalent SMOS value from 155
 an AMSR-E observation. This high correlation implies that the 156
 occurrence of precipitation between the SMOS and AMSR-E 157
 overpasses is rare. Moreover, it is well known that soil moisture 158
 has a long temporal correlation time scale, so the overpass time 159
 differences will have a minimal effect on the analysis. 160

The impact of the different frequencies between AMSR-E 161
 and SMOS is, in most situations, not significant. The higher 162
 AMSR-E frequency (10.7 GHz) results in a more superficial 163
 emission depth than the SMOS observations, so while the 164
 retrieved values may be different, their relative values will be 165
 similar (both dry or wet). The correlation between paired ob- 166
 servations depends on their relative values (with their individual 167
 time series) and not absolute values, and in the case of copula- 168
 based joint distributions, the correlation is represented by the 169
 Kendall tau whose calculation is based on ranks. 170

If the two sensing depths were to be reconciled physically, 171
 given the soil property variability (spatially and with depth) 172
 with different wetting and drying properties, a physical model 173
 would introduce significant uncertainty that could be very 174
 difficult to estimate afterward. If the SMOS (or AMSR-E) 175
 data were adjusted to the AMSR-E (or SMOS) emission depth 176
 through data assimilation into a land surface model for exam- 177
 ple, then the complete record would have to be adjusted with 178
 the added uncertainty of the data assimilation step. With any 179
 of the suggested adjustments, there is a mismatch with the 180
 past or with the future. Only by treating the original data sets 181
 and determining the information content between them can a 182
 consistent approach be represented. 183

Data assimilation could, however, deal with the precipitation 184
 and the difference in sensing depth issues, but that would imply 185
 other uncertainties such as the space–time variability of the 186
 precipitation data sets, as well as other meteorological issues. 187
 Building a homogeneous time series based on data assimila- 188
 tion into a land surface model can be seen as a competing 189
 approach. 190

In this paper, we show two statistical methods to obtain 191
 this homogeneous time series. The satellite data and the four 192
 watersheds where the time series are simulated are presented 193
 in Section II. The two statistical methods for generating ho- 194
 mogeneous time series are presented in Section III which 195
 includes the general theory and how to apply them to real data. 196
 Simulated time series over the four watersheds are presented in 197
 Section IV. Conclusions and perspectives are described in the 198
 last section. 199

200 II. REGIONS OF INTEREST AND SATELLITE DATA

201 A. SMOS

202 With its L-band radiometer, SMOS [4] has been providing
 203 soil moisture data for almost three years and global coverage
 204 every three days with a 43-km resolution. The satellite is polar
 205 orbiting with equator crossing times of 6 am (local solar time
 206 (LST), ascending) and 6 pm (LST, descending). The signal at
 207 L-band is mainly influenced by the water content at the surface
 208 of the soil (around 5 cm).

209 SMOS acquires brightness temperatures at multiple inci-
 210 dence angles, from 0° to 55° with full polarization. The an-
 211 gular signature is a key element of the retrieval algorithm
 212 that provides soil moisture and the vegetation optical thickness
 213 through the minimization of a cost function between modeled
 214 and acquired brightness temperatures [33], [34]. This estimated
 215 soil moisture is referred as the Level 2 product [34] and is
 216 available on the Icosahedral Snyder Equal Area-4h9 grid [35].
 217 The nodes of this grid are equally spaced at about 15 km. In
 218 this paper, the 2010 SMOS Level 2 version 4 products have
 219 been used.

220 Currently, numerous studies are underway on the validation
 221 of SMOS soil moisture product with *in situ* measurements
 222 and estimates of other sensors and models. Bitar *et al.* [36]
 223 used the Soil Climate Analysis Network [37] and the Snow-
 224 pack Telemetry sites in North America to compare SMOS
 225 soil moisture retrievals and ground measurements. That study
 226 showed that SMOS soil moisture had a very good dynamic
 227 response but tended to underestimate the values. However,
 228 the new version of the product (V4) significantly improved
 229 the general results. Jackson *et al.* [38] studied SMOS soil
 230 moisture and vegetation optical depth over four watersheds in
 231 the U.S. They concluded that SMOS almost met the accuracy
 232 requirement with root-mean-square errors (rmse) of 0.043 and
 233 0.047 m³/m³ in the morning and afternoon, respectively,
 234 whereas the vegetation optical depth retrievals were not reliable
 235 yet for use in vegetation analyses. Leroux *et al.* [39] compared
 236 SMOS data with other satellite and model output products over
 237 the same four watersheds for the year 2010. It showed that
 238 SMOS soil moisture data were closer to the ground measure-
 239 ments than the other data sets. Even though the correlation
 240 coefficient was not the best, the bias was extremely small.

241 After the results of the validation activities, the European
 242 Center for Medium-Range Weather Forecasts has decided and
 243 is now ready to process SMOS data in near real time into their
 244 Integrated Forecast System. It is expected to have an impact on
 245 the weather forecast at short and medium ranges [40].

246 B. AMSR-E

247 The AMSR-E was launched in June 2002 on the Aqua
 248 satellite. This radiometer acquires data with a single 55° inci-
 249 dence angle at six different frequencies: 6.9, 10.7, 18.7, 23.8,
 250 36.5, and 89.0 GHz, all dual polarized. The crossing times are
 251 respectively 1:30 am (LST, descending) and 1:30 pm (LST,
 252 ascending).

253 There are several soil moisture products available that are
 254 based on AMSR-E data. Many studies have already showed

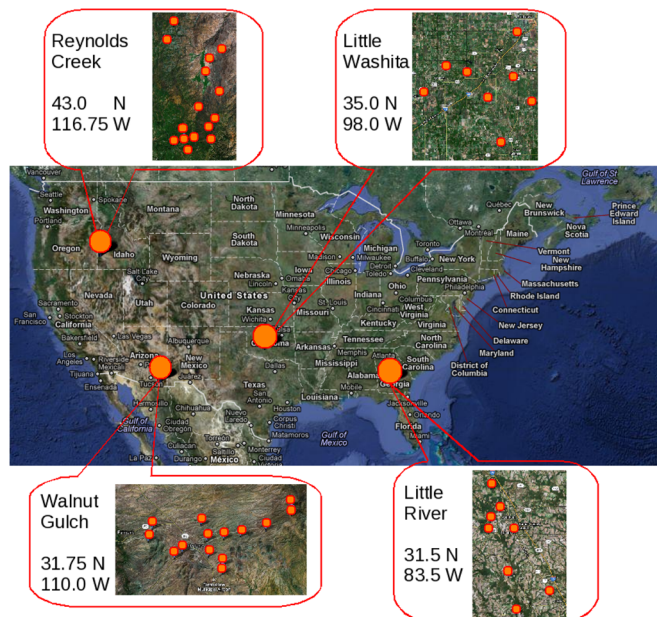


Fig. 1. Map of the four sites: WG, AZ; LW, OK; LR, GA; and RC, ID.

that the NASA product [41] is not able to reproduce low values
 of soil moisture and has low dynamic range [42]–[46]. The
 soil moisture data produced by the joint collaboration of the
 Vrije University of Amsterdam and NASA (whereafter called
 the Land Parameter Retrieval Model (LPRM) [7]) were chosen
 in this study.

The LPRM [7] retrieves soil moisture and optical thickness
 using the C- and X-band AMSR-E channels (combined prod-
 uct) and 36.5 GHz to estimate the surface temperature. This
 algorithm is based on a microwave radiative transfer model with
a priori information about soil characteristics. The products are
 available on a 0.25° × 0.25° grid only for the descending orbit.
 These data have been quality controlled, and the contaminated
 estimates due to high topography and extreme weather condi-
 tions such as snow have been flagged and not been considered
 in this study.

C. Study Areas

Four watersheds located in the United States were selected
 for this study: Walnut Gulch (WG) in Arizona, Little Washita
 (LW) in Oklahoma, Little River (LR) in Georgia, and Reynolds
 Creek (RC) in Idaho (see Fig. 1). They represent different
 types of climate (from semiarid to humid) and land use patterns
 [47]. These four watersheds have been used as calibration and
 validation sites for comparison of AMSR-E satellite product
 [47] and SMOS product [38], [39].

WG is located in the Southeast Arizona. Most of the water-
 shed is covered by shrubs and grass, which is typical of the re-
 gion. The annual mean temperature is 17.6 °C (at Tombstone),
 and the annual mean precipitation is 320 mm (mainly from
 high intensity convective thunderstorms in the late summer).
 The uppermost 10 cm of the soil profile contains up to 60%
 gravel, and the underlying horizons usually contain less than
 40% gravel.

TABLE I
WATERSHED CHARACTERISTICS AND THE COORDINATES OF THE BOX CONTAINING THE POINTS USED FOR STATISTICS

Watershed	Number of stations	Climate	Annual rainfall (mm)	Topography	Land use	Box for statistics (corners coord.)
Walnut Gulch AZ	14	semi-arid	320	rolling	range	31.3 N - 110.5 W 32.3 N - 109.5 W
Little Washita OK	8	sub-humid	750	rolling	range/wheat	34.4 N - 98.5 W 35.4 N - 97.5 W
Little River GA	8	humid	1200	flat	row crop/forest	31.0 N - 84.0 W 32.0 N - 83.0 W
Reynolds Creek ID	15	semi-arid	500	mountainous	range	34.7 N - 98.7 W 35.7 N - 97.7 W

TABLE II
CORRELATION COEFFICIENTS (R) BETWEEN THE IN SITU MEASUREMENTS AT 130 AM AND 600 AM FOR THE FOUR WATERSHEDS. N IS THE NUMBER OF AVAILABLE DATES, AND CI IS THE 95% CONFIDENCE INTERVAL

WG			LW		
R	N	CI	R	N	CI
0.96	365	[0.95-0.97]	0.97	365	[0.96-0.98]
LR			RC		
R	N	CI	R	N	CI
0.95	365	[0.94-0.96]	0.99	328	[0.99-0.99]

288 LW is located in Southwest Oklahoma in the Southern Great
289 Plains region of the U.S. The climate is subhumid with an
290 average annual rainfall of 750 mm (mainly during the spring
291 and fall seasons). Topography is moderately rolling with a
292 maximum relief of less than 200 m. Land use is dominated by
293 rangeland and pasture (63%).

294 LR is located in the Southern Georgia near Tifton. With
295 an average annual precipitation of 1200 mm, the climate is
296 humid. The LR watershed is typical of the heavily vegetated
297 slow-moving stream systems in the Coastal Plain region of
298 the U.S. The topography over this watershed is relatively flat.
299 Approximately 40% of the watershed is forest with 40% crops
300 and 15% pasture.

301 RC is located in a mountainous area of Southwest Idaho. The
302 topography is high with a relief of over 1000 m that results in
303 diverse climates. Soils and vegetations are typical in this part
304 of the Rocky Mountains. The climate is considered as semiarid
305 with an annual precipitation of 500 mm. Approximately 75% of
306 the annual precipitation at high elevation is snow, whereas only
307 25% is snow at low elevation.

308 Surface soil moisture and temperature sensors (0–5 cm) have
309 been acquiring data since 2002 for the four watersheds. The
310 data used in this study are the means and standard deviations
311 of the soil moisture and surface temperature acquired every
312 30 min from 2009 to 2010 (hourly for RC). The averages
313 are based on 14/8/8/15 sensors for WG/LW/LR/RC, respec-
314 tively, after eliminating sensors with poor and suspicious
315 performances. Weighting coefficients have been derived for
316 each sensor with a Thiessen polygon. Table I summarizes the
317 characteristics of each watershed [47].

318 In order to estimate the effect of the rainfalls that could
319 occur between 130 am and 600 am, the correlation coefficients
320 between the measurements at 130 am and 600 am have been
321 computed for the four watersheds (see Table II and Fig. 2). They
322 range from 0.95 to 0.99, and based on the fact that rainfalls
323 would lower the correlation, we can assess that precipitations
324 that do not affect significantly the analysis.

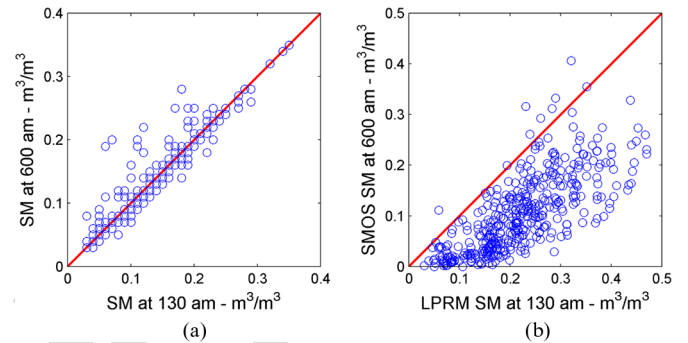


Fig. 2. Comparison between the 130 am and the 600 am soil moisture: *In situ* observations and satellite products for the four watersheds. (a) *In situ* soil moisture at 130 am and 600 am. (b) LPRM (130 am) and SMOS (600 am) soil moisture.

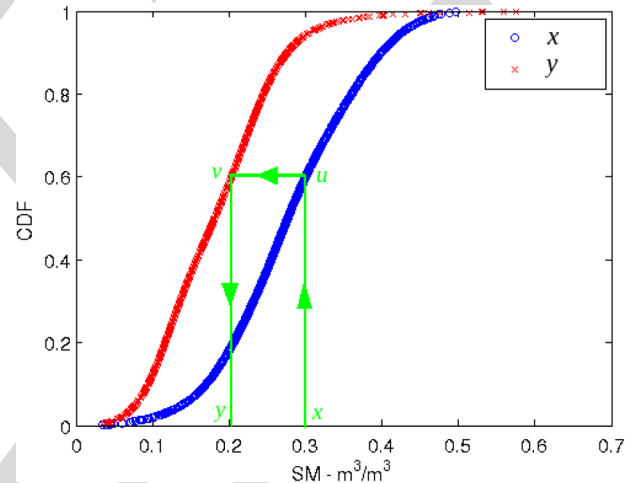


Fig. 3. Principle of CDF matching by setting the probabilities equal. For a given x , find y such that $G_Y(y) = F_X(x)$.

III. TWO STATISTICAL METHODS FOR GENERATING HOMOGENEOUS TIME SERIES 325 326

Two statistical methods were used to create a homogeneous 327 time series of soil moisture. CDF matching has been widely 328 used in previous studies to merge time series [14], [15], [18], 329 [19], whereas copulas have just started to be used recently for 330 environmental purposes. 331

A. CDF Matching 332

The CDF is the probability that a random variable X takes a 333 value less than or equal to a given number x 334

$$F_X(x) = \Pr[X \leq x] \quad (1)$$

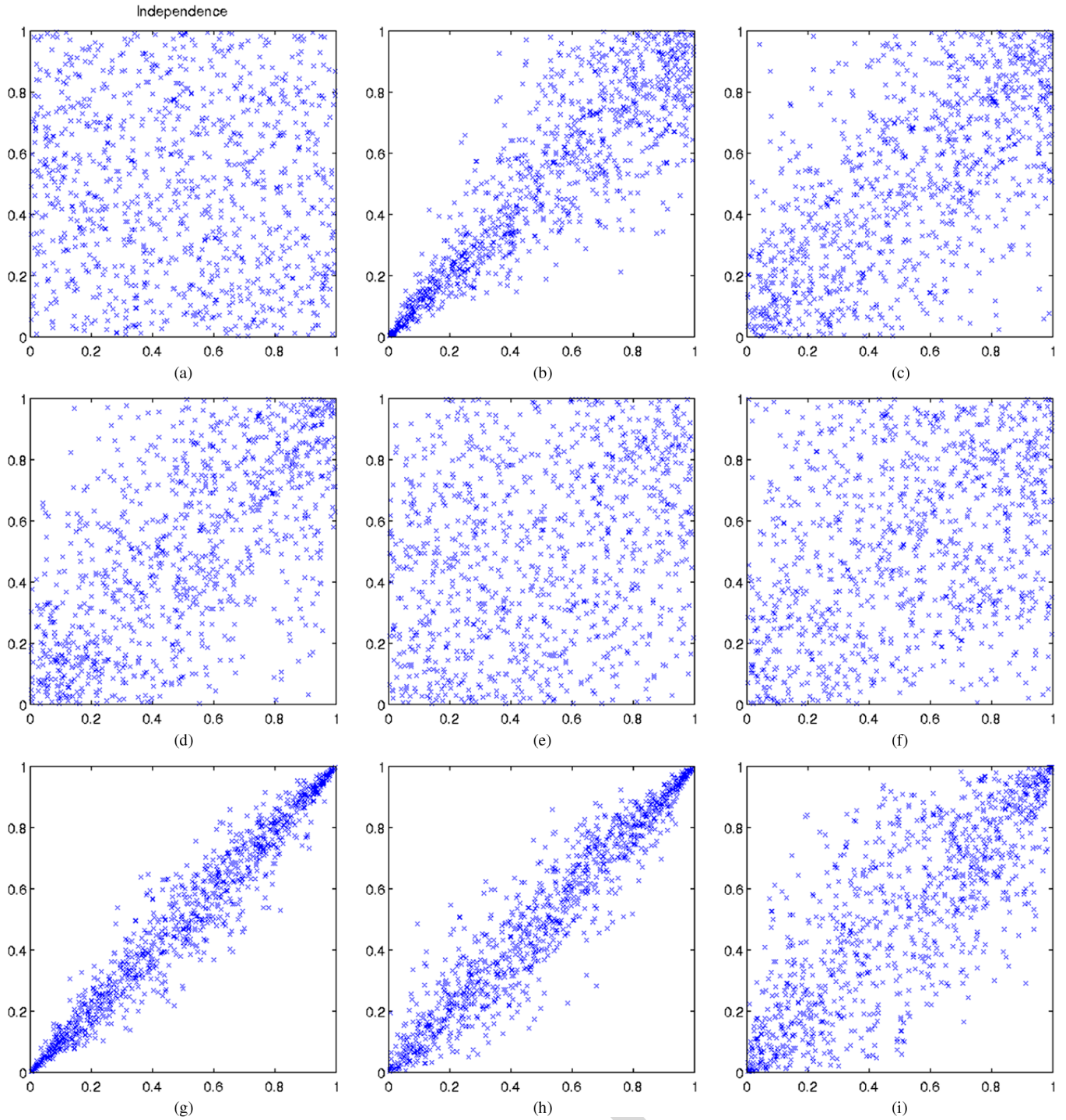


Fig. 4. Representations of the nine copulas showing their characteristics in the form of the point cloud (x -axis: CDF of the first data set; y -axis: CDF of the second data set).

335 where F_X is the CDF of the random variable X . If two time
 336 series are considered, the CDF matching consists of matching
 337 the CDF of each data set by setting their probabilities equal
 338 (see Fig. 3). The following approach has been applied here to
 339 the soil moisture data.

- 340 1) Compute the CDF of both data sets X and Y : F_X and G_Y .
- 341 2) Given a value x of X , find y such that $G_Y(y) = F_X(x)$.

342 However, the assumption that the probabilities $F_X(x)$ and
 343 $G_Y(y)$ are equal is never confirmed, and most of the time, they

are scattered like in Fig. 4. The copula method models this
 344 dependence between the probabilities. 345

For the rest of this paper, we use the variable u to represent
 346 $F_X(x)$ and v for $G_Y(y)$. U and V are data sets, whereas u and
 347 v are values of these data sets. 348

B. Copulas 349

The copula theory is a very useful and powerful tool to model
 350 the dependence structure between two sets of random variables. 351

TABLE III
NINE COPULAS TESTED IN THE STUDY: DEFINITION, PARAMETER RANGE, AND FAMILY

Copula	$C_\theta(u, v)$	$\theta \in$	Family
Independent	$u \cdot v$	-	-
Clayton	$(u^{-\theta} + v^{-\theta} - 1)^{-1/\theta}$	$(0, \infty)$	Archimedean
Frank	$-\frac{1}{\theta} \ln \left(1 + \frac{(e^{-\theta u} - 1)(e^{-\theta v} - 1)}{e^{-\theta} - 1} \right)$	$(-\infty, \infty)/0$	Archimedean
Gumbel	$\exp \left(- \left((-\ln u)^\theta + (-\ln v)^\theta \right)^{1/\theta} \right)$	$[1, \infty)$	Archimedean
FGM	$uv + \theta uv(1-u)(1-v)$	$[-1, 1]$	Elliptical
AMH	$\frac{uv}{1 - \theta(1-u)(1-v)}$	$[-1, 1]$	Archimedean
Arch12	$\left(1 + \left((u^{-1} - 1)^\theta + (v^{-1} - 1)^\theta \right)^{1/\theta} \right)^{-1}$	$[1, \infty)$	Archimedean
Arch14	$\left(1 + \left((u^{-1/\theta} - 1)^\theta + (v^{-1/\theta} - 1)^\theta \right)^{1/\theta} \right)^{-1/\theta}$	$[1, \infty)$	Archimedean
Gaussian	$\frac{\int_{-\infty}^{\phi^{-1}(u)} \int_{-\infty}^{\phi^{-1}(v)} \exp \left(\frac{2\theta s\omega - s^2 - \omega^2}{2(1-\theta^2)} \right)}{2\pi\sqrt{1-\theta^2}}$	$[-1, 1]$	Elliptical

352 Like the CDF matching, copulas separate the marginal behavior
353 of variables from the dependence structure by using distribution
354 functions. Instead of setting the probabilities u and v equal,
355 the variables U and V are compared and analyzed. The copula
356 function binds the two variables together.

357 There are many families of copulas which exhibit very differ-
358 ent properties. The form of the scatter of U and V is controlled
359 by the family choice, and the width of the tail of this scatter
360 is controlled by the single parameter θ . Most of the definitions
361 that follow in this section are based on [21].

362 1) *General Theory*: A copula is a function that gener-
363 ates a multivariate cumulative distribution function from 1-D
364 marginal CDFs. Given two random variables, X and Y , with
365 marginal CDFs F_X and G_Y , then, Sklar's theorem states

$$H_{XY}(x, y) = C_{XY}(F_X(x), G_Y(y)) = \Pr[X \leq x, Y \leq y] \quad (2)$$

366 where H_{XY} is the joint CDF of X and Y and C_{XY} is the asso-
367 ciated copula function. It is then possible to derive conditional
368 distributions, $H_{XY}(y|x)$, i.e., the joint CDF knowing x . Let
369 $u = F_X(x)$ and $v = G_Y(y)$. Then, $H_{XY}(y|x)$ can be derived by

$$C_{V|U} = \frac{\partial C(u, v)}{\partial u}. \quad (3)$$

370 Schweizer and Wolff [48] established that the copula func-
371 tion accounts for all the dependence between the two variables.
372 They demonstrated that transformations of the variables X and
373 Y do not affect their associated variables. Thus, the way that X
374 and Y evolve together is captured by the copula, regardless of
375 the scale in which each variable is measured.

376 2) *Some Copula Families*: The product copula corresponds
377 to the independence between X and Y

$$C(u, v) = u \cdot v. \quad (4)$$

378 A copula of the Archimedean family takes the following
379 form:

$$C(u, v) = \phi^{-1}(\phi(u) + \phi(v)) \quad (5)$$

380 where ϕ is the generator function that goes from $[0, 1]$ to
381 $(0, \infty)$. It satisfies three conditions: $\phi(1) = 0$, ϕ strictly de-
382 creasing, and ϕ convex.

383 Elliptical copulas have distributions with elliptic contours.
384 The main advantage of elliptical distributions is that the level

of correlation between the variables U and V can be specified. 385
The disadvantages are that elliptical copulas do not have closed- 386
form expressions and are restricted to have radial symmetry. 387

In this paper, nine copulas were used: the product cop- 388
ula, Clayton, Frank, Gumbel, Farlie–Gumbel–Moregenstern 389
(FGM), Ali–Mikhail–Haq, Arch12 (the 12th copula presented 390
in [21]), Arch14 (the 14th copula presented in [21]), and the 391
Gaussian copula. The nine copulas are described in Table III 392
and Fig. 4 and have their own characteristics. 393

- 1) Clayton: Strong left tail dependence and relatively weak 394
right tail dependence (i.e., u and v are strongly linked for 395
low values, whereas they are not for high values). 396
- 2) Frank: Dependence is symmetric in both tails, weak in 397
both tails, and stronger in the center of the distribution. 398
- 3) Gumbel: Strong right tail dependence and relatively weak 399
left tail dependence (the opposite of Clayton). 400
- 4) FGM: Useful when the dependence between U and V is 401
modest in amplitude. 402
- 5) Gaussian: Flexible as it allows for positive and negative 403
dependences. 404

Hafner and Reznikova [23] and Wang and Pham [49] 405
developed a method that includes the time into the copula 406
formula to create a dynamic copula evolving with time. In 407
this paper, time was not included, but the year 2010 was 408
divided into four seasons as different statistical behaviors were 409
expected: December–January–February, March–April–May 410
(MAM), June–July–August (JJA), and September–October– 411
November (SON). 412

3) *How to Select a Family*: Since copulas separate marginal 413
distributions from dependence structures, the appropriate cop- 414
ula for a particular application is the one that best captures the 415
dependence features of the data [22]. Dupuis [27] examined the 416
effects of model misspecification and highlighted the dangers 417
of improper copula selection. Genest and Rivest [50] proposed 418
a method to select the most appropriate copula, but this method 419
is only relevant for Archimedean copulas. Other methods 420
were developed to compare any type of copulas [51]–[54]. 421
Genest *et al.* [55] and Berg [54] compared some of them 422
and concluded that there was no universal test and that some 423
procedures performed better in some situations but never in all 424
the situations. 425

426 The method proposed by Huard *et al.* [56] is based on a
 427 Bayesian approach where any type of copula can be tested. It
 428 does not perform perfectly well in all the situations (with small
 429 correlation coefficients or with small sample size) but has the
 430 advantage to be a very fast method. This method was chosen
 431 in this study to select the copula that provides the best fit to the
 432 data.

433 4) *Method Used for Simulations:* The key to generating
 434 simulations from a copula is to understand that a copula is a
 435 joint distribution and that it obeys to the same rules. A con-
 436 ditional copula $C_{V|U}(u, v)$ is the probability that the random
 437 variable V is less than or equal to a value v knowing that the
 438 random variable U is equal to a value u

$$C_{V|U}(u, v) = \Pr[V \leq v | U = u] = t \sim \mathcal{U}(0, 1). \quad (6)$$

439 Simulating a uniform variable t is necessary in order to
 440 generate simulations from a copula. To retrieve $V|U$, the func-
 441 tion $C_{V|U}$ needs to be inverted such that $v = C_{V|U}^{-1}(t)$, or the
 442 equation $C_{V|U}(v) = t$ needs to be solved numerically. For each
 443 value of t , a value for v is retrieved. The following approach
 444 was used here to simulate data with the copulas.

- 445 1) Compute F_X and G_Y from the two original data sets X
 446 and Y with (1).
- 447 2) Choose the appropriate copula C by applying Huard's
 448 method and fitting the parameter θ to the original data.
- 449 3) Derive the conditional copula $C_{V|U}$ with (3).
- 450 4) Generate 1000 simulations $t \sim \mathcal{U}(0, 1)$.
- 451 5) Compute v with $v = C_{V|U}^{-1}(t)$ and y with $y = G_Y^{-1}(v)$.
- 452 6) The mean and standard deviation from the 1000 simu-
 453 lations can be computed.

454 IV. METHODOLOGY

455 For the CDF matching and the copula methods, 2010 data
 456 were used for calibration. The CDFs of SMOS and LPRM were
 457 calculated for the 2010 data sets. The two algorithms were then
 458 applied to the data from previous years. It should be noted that
 459 the consequence of using 2010 as a calibration year is that only
 460 the soil moisture range from 2010 is taken into account. If an
 461 extreme event occurred in the previous years, it might not be
 462 well described with these methods as they are only based on
 463 statistics and not on physical models. By looking at the *in situ*
 464 soil moisture time series in Fig. 7, 2010 did not have enough
 465 wet values over LR to estimate correctly the strong rainfalls
 466 of 2004, 2005, and 2009, not enough wet values over LW for
 467 rainfalls in 2007 and not enough dry values as well for 2003
 468 and 2006, and again not enough dry values over RC for all the
 469 previous years.

470 The two methods were applied to data contained in a $1^\circ \times 1^\circ$
 471 box around each watershed in order to have enough points for
 472 computing reliable statistics. The coordinates of each box are
 473 indicated in Table I. Only the satellite morning overpasses were
 474 selected for this study (6:00 am for SMOS and 1:30 am for
 475 AMSR-E, LST) since LPRM retrievals were only available for
 476 this overpass.

477 The 2010 calibration year was divided into four seasons:
 478 December–January–February, MAM, JJA, and SON. This

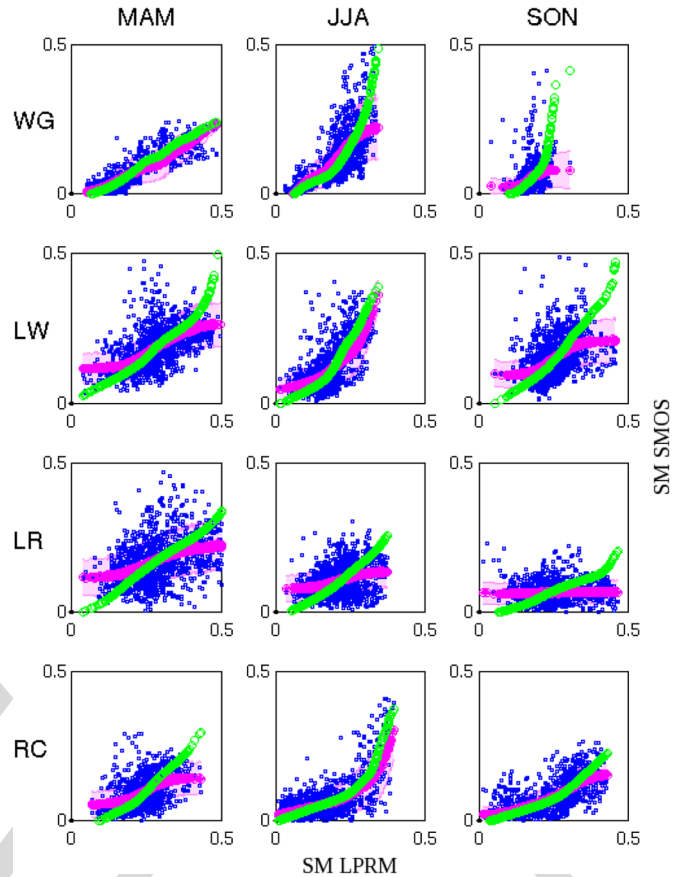


Fig. 5. Discrepancies in the simulations of soil moisture between CDF matching and copulas in 2010. Original soil moisture LPRM data are represented by blue points, and simulated data with CDF matching and copulas are in green and red, respectively. The standard deviation of the copula simulations is represented in shadowed red. Each row corresponds to a site, and each column corresponds to a season. *x*-axis: LPRM soil moisture. *y*-axis: SMOS soil moisture.

subdivision was done in order to better capture the sea-
 479 sonal dynamic that can be very different depending on the
 480 time of the year, particularly in vegetated areas. However,
 481 not enough points were available during the winter period
 482 (December–January–February) to compute reliable statistics,
 483 so no estimation was performed for this season. 484

When comparing either two different remote sensing prod-
 485 ucts or *in situ* data with remote sensing products, there is the
 486 issue of the scale effect, as the products may have significantly
 487 different spatial resolutions. Moreover, the spatial variability
 488 varies with the seasons and the heterogeneity. So as to reduce
 489 the problem, we used in this study averaged *in situ* data sets
 490 (8 to 15 stations that were several miles away) which were
 491 especially produced to be representative of 50-km spatial res-
 492 olution or so [47]. Also, statistics were applied to all the points
 493 contained in a $1^\circ \times 1^\circ$ box (more than 50 grid points). 494

495 V. GENERATED HOMOGENEOUS TIME SERIES

The year 2010 was used to compute the CDFs of each
 496 data set (SMOS and LPRM) for both methods and the joint
 497 CDF based on fitting and selecting copula functions as de-
 498 scribed previously. The soil moisture data were estimated using 499

TABLE IV
STATISTICAL RESULTS OF THE SIMULATIONS FROM COPULAS AND CDF MATCHING. THE SIMULATIONS WERE COMPARED TO GROUND MEASUREMENTS OVER 2010 DIVIDED INTO FOUR SEASONS: MAM, JJA, SON, BUT NOT ENOUGH DATA AVAILABLE FOR WINTER SEASON. THE BEST RESULTS ARE WRITTEN IN BOLD, AND RMSES ARE IN m^3/m^3

		SMOS		LPRM		Copula method			CDF matching		# points
		R	RMSE	R	RMSE	Fam(θ)	R	RMSE	R	RMSE	
WG	MAM	0.80	0.032	0.82	0.125	Gumbel (2.18)	0.89	0.020	0.87	0.031	43
	JJA	0.86	0.053	0.86	0.126	Clayton(2.63)	0.76	0.076	0.81	0.090	45
	SON	0.64	0.029	0.79	0.133	Frank (3.13)	0.64	0.012	0.53	0.029	42
	total	0.84	0.040	0.79	0.139	-	0.79	0.043	0.82	0.054	159
LW	MAM	0.70	0.068	0.48	0.166	Frank (4.40)	0.55	0.057	0.57	0.075	44
	JJA	0.85	0.037	0.58	0.085	Gumbel (1.66)	0.77	0.042	0.76	0.050	44
	SON	0.80	0.041	0.80	0.122	Frank (3.61)	0.75	0.023	0.72	0.048	46
	total	0.78	0.049	0.59	0.148	-	0.71	0.043	0.71	0.059	162
LR	MAM	0.77	0.080	0.54	0.175	Frank (2.82)	0.59	0.063	0.58	0.067	39
	JJA	0.57	0.053	0.67	0.131	Frank (2.00)	0.65	0.034	0.66	0.033	40
	SON	0.59	0.032	0.37	0.174	FGM (0.31)	0.17	0.033	0.16	0.037	39
	total	0.74	0.060	0.65	0.178	-	0.51	0.045	0.59	0.048	147
RC	MAM	0.14	0.097	0.11	0.096	Frank (3.10)	0.26	0.089	0.27	0.105	47
	JJA	0.63	0.055	0.81	0.070	Gumbel (1.81)	0.84	0.047	0.83	0.052	42
	SON	0.14	0.070	0.52	0.144	Frank (6.30)	0.34	0.056	0.29	0.066	39
	total	0.55	0.081	0.73	0.099	-	0.80	0.059	0.70	0.067	142

500 the conditional distribution (conditional on LPRM retrievals).
501 While the copula procedure has the potential to generate an
502 ensemble of SMOS-like soil moisture estimates, given the
503 LPRM estimated soil moisture, we only use the mean estimate.
504 The ensembles could be used to provide uncertainty estimates.
505 It should be noted that CDF matching can only provide a
506 single SMOS estimate. The resulting time series will result in
507 a statistically homogeneous time series under the assumption
508 that 2010 LPRM retrievals and the underlying AMSR-E bright-
509 ness temperatures are temporally consistent. The resulting
510 SMOS-like estimated soil moisture is then compared to ground
511 measurements.

512 A. Calibration Year 2010 and Comparison With 513 Ground Measurements

514 2010 is the year with both SMOS data and LPRM data.
515 CDFs were computed for both variables. CDF matching and
516 copula methods were then applied, and these produced different
517 SMOS-like estimates. In Fig. 5, the original data (SMOS and
518 LPRM) are represented by the blue point cloud, CDF matching
519 and copula estimates are in green and red colors, respectively,
520 and standard deviations from copula simulations are in red
521 shadows. This standard deviation can be interpreted as the
522 uncertainty associated to the copula simulations, which can be
523 not produced by CDF matching estimation.

524 Over WG in the MAM season, there was no obvious differ-
525 ence between the two simulation methods. However, in the JJA
526 and SON seasons, there were differences for the high values
527 of soil moisture: The CDF matching method produced higher
528 simulated values than the copula method. Similar behavior can
529 also be seen for all seasons in the other three sites, i.e., LW, LR,
530 and RC. Discrepancies can also be observed for small values
531 of soil moisture over LW, LR, and RC (MAM) where copulas
532 generated higher values of soil moisture.

533 Standard deviations of soil moisture simulations from copu-
534 las were also computed (see Fig. 5). This standard deviation is
535 directly related to the width of the tail of the chosen copula
536 which is controlled by the θ parameter. A high value of the
537 standard deviation corresponds to a large tail, meaning that

the two variables are weakly linked to each other, whereas a 538
small value corresponds to a strong link. The differences in 539
the simulations can also be observed in the 2010 time series 540
(see Table IV and Fig. 6). Compared to the original LPRM 541
data, the estimated soil moisture was close to the SMOS level 542
and comparable to the ground measurements. The bias between 543
LPRM and SMOS was corrected by both methods. 544

Over WG, CDF matching and copula simulations were not 545
very different except in the summer season when the CDF 546
matching simulations were higher than the copulas. Consid- 547
ering the entire year, both simulation methods improved the 548
original statistics from the LPRM data set. The correlation 549
coefficient did not change significantly ($R = 0.79$ for LPRM 550
and $R = 0.79/0.82$ for copulas/CDF matching), but the rmse 551
was highly improved going from $0.139 \text{ m}^3/\text{m}^3$ (original LPRM 552
data) to $0.054 \text{ m}^3/\text{m}^3$ with CDF matching and $0.043 \text{ m}^3/\text{m}^3$ 553
with copula, which represents an improvement of a factor of 3. 554

Over LW, simulations responded very well to the succes- 555
sive rain events throughout the year and exhibited a pattern 556
of decrease following a rain event. The first two months 557
(March–April) exhibited more noisy simulations, and the statis- 558
tics were impacted by this behavior ($R = 0.55/0.57$ and 559
 $\text{rmse} = 0.057/0.075 \text{ m}^3/\text{m}^3$ for copulas/CDF matching). The 560
other two seasons gave good results in terms of statistics. For 561
the entire year, the R value was highly improved ($R = 0.59$ 562
for LPRM and $R = 0.71/0.71$ for copulas/CDF matching), and 563
the rmse was reduced by a factor of 3 ($\text{rmse} = 0.148 \text{ m}^3/\text{m}^3$ 564
for LPRM and $\text{rmse} = 0.043/0.059 \text{ m}^3/\text{m}^3$ for copulas/CDF 565
matching). 566

The LR watershed is the site with the highest rainfall fre- 567
quency (events of small amplitude). The successive rainfall 568
events were not well captured by the simulations, particularly 569
during the fall season when both simulations exhibited only 570
small variations, which resulted in very poor statistics ($R =$ 571
 $0.17/0.16$ for copulas/CDF matching). Unfortunately, even if 572
the rain events were captured by the original data sets, none 573
was captured by both data sets at the same time, so only the 574
nonraining periods were taken into account by the statistics. 575
Therefore, the simulations can only be representative of the dry 576
periods. It should be noted that the statistics of LPRM were 577

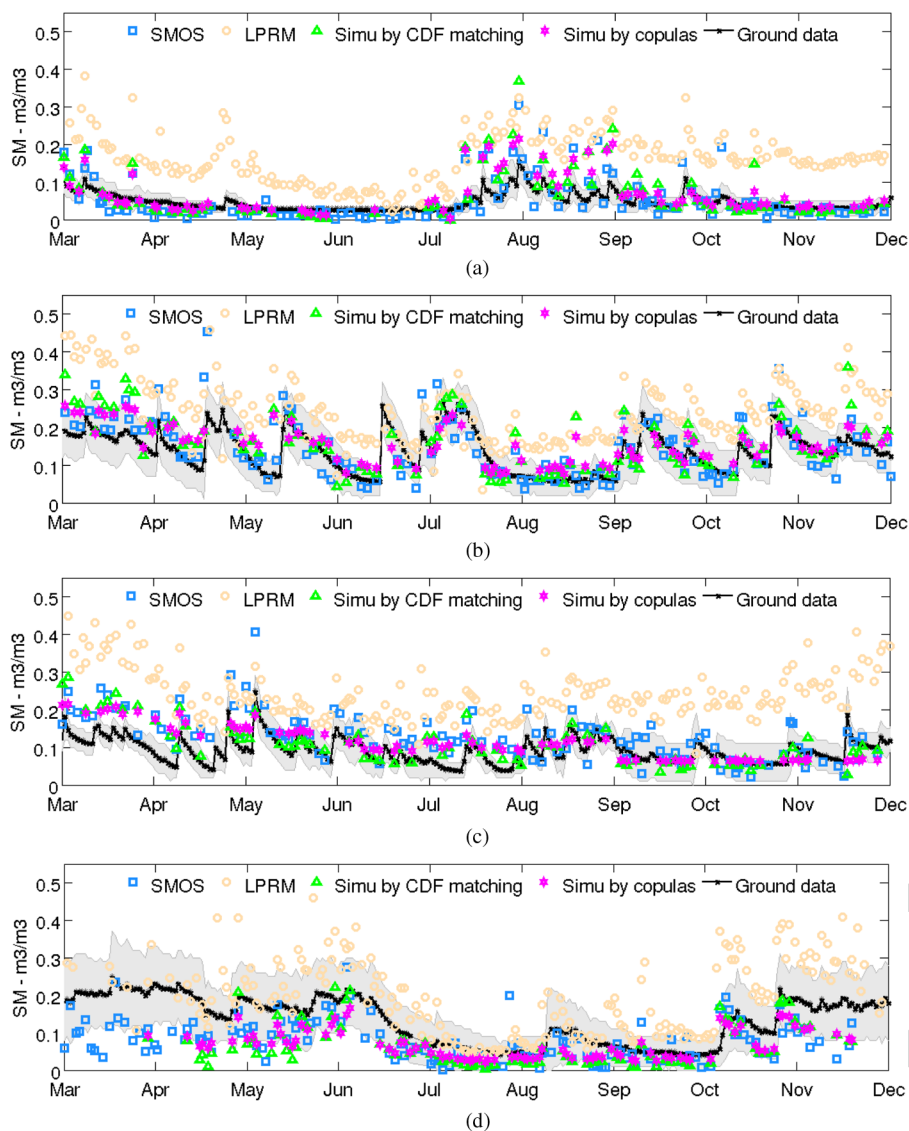


Fig. 6. Simulations for 2010: SMOS, LPRM, simulated soil moisture data from CDF matching and copulas, and ground measurements over the four watersheds. Since the *in situ* data are the mean of several ground measurements, their standard deviations are represented in gray shadows showing the spatial variability. (a) WG. (b) LW. (c) LR. (d) RC.

578 already not good during this season ($R = 0.37$ and $rmse =$
 579 $0.174 \text{ m}^3/\text{m}^3$). During the spring season, SMOS overestimated
 580 the *in situ* soil moisture measurements, so as a result, the
 581 copulas and CDF matching estimates overestimated the *in situ*
 582 measurements as well.

583 RC is located in a mountainous region and is subject to
 584 frequent snow and frozen soil events. The satellite-based soil
 585 moisture was not comparable to the ground measurements until
 586 late May. After this winter period, the simulations captured
 587 accurately the soil moisture evolution and improved the original
 588 statistics and especially the $rmse$ ($0.099 \text{ m}^3/\text{m}^3$ for LPRM and
 589 $0.059/0.067 \text{ m}^3/\text{m}^3$ for copulas/CDF matching).

590 *B. Times Series 2003–2010 and Comparison With*
 591 *Ground Measurements*

592 Soil moisture from 2003 to 2010 was simulated from the
 593 LPRM retrievals (2003–2010) using the copulas and CDF

matching relationships developed for 2010. Fig. 7 and Table V
 594 show the entire time series and the associated statistics (R and
 595 $rmse$) between the original data, CDF matching simulations,
 596 copula simulations, and ground measurements. 597

WG is the driest site and did not have a lot of rain events.
 598 These rain events were well described by the simulated soil
 599 moisture even though they were sometimes largely overesti-
 600 mated, particularly by CDF matching simulations. Artifacts at
 601 the extremities of the seasons can be seen at the beginning
 602 of 2006 and 2008. The correlation coefficient was improved
 603 using the CDF matching for each year, whereas the errors were
 604 reduced by a factor larger than 2 with the copulas. 605

The overestimation of the soil moisture after the rain events
 606 with CDF matching can be found as well over LW, but the
 607 temporal evolution was well captured by both methods. For this
 608 watershed, CDF matching overestimated the high soil moisture
 609 values and underestimated the low values. CDF matching pro-
 610 duced soil moisture with a higher dynamic range than copulas.
 611

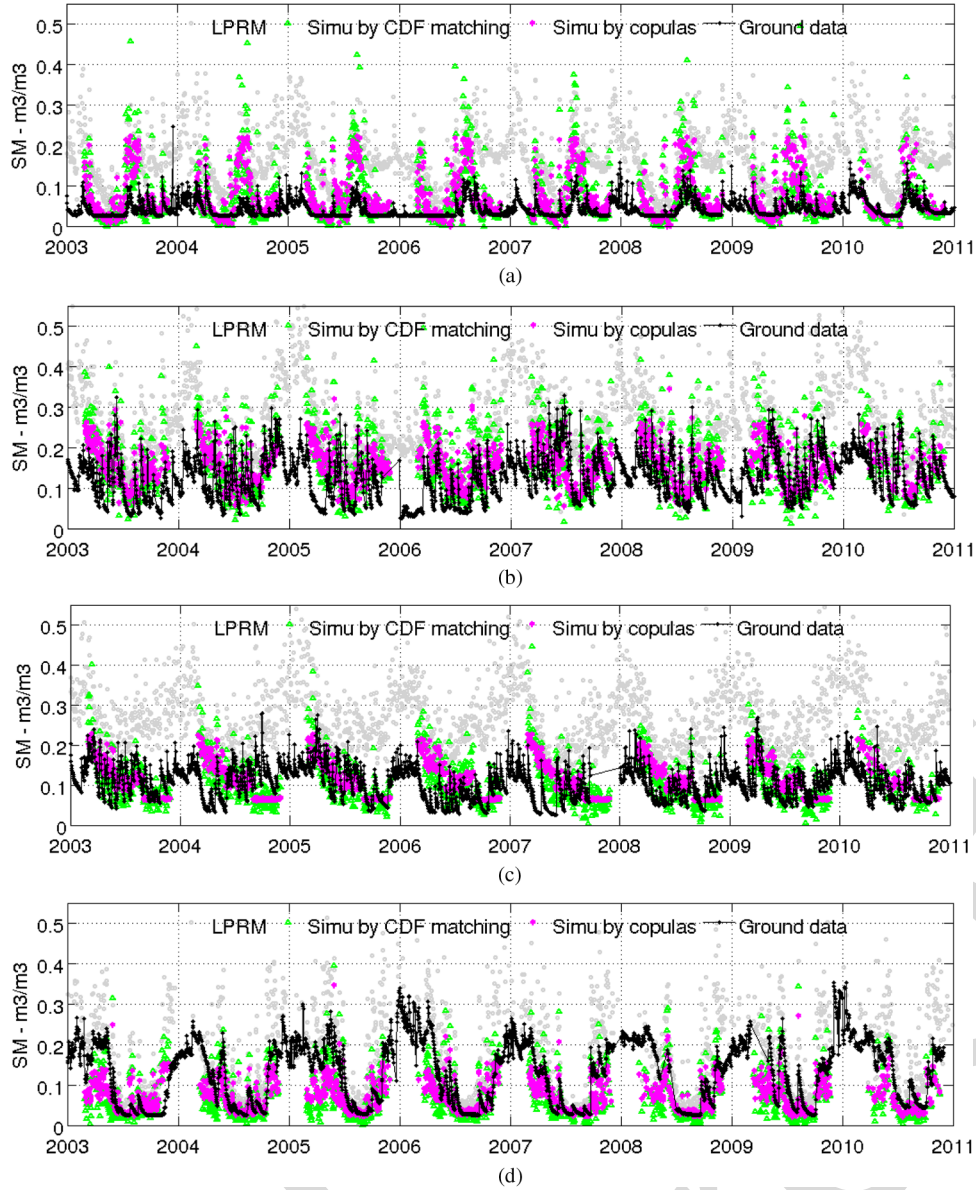


Fig. 7. Simulated time series from 2003 to 2010 with ground measurements for the four watersheds. (a) WG. (b) LW. (c) LR. (d) RC.

612 This was reflected in the total rmse value ($0.079 \text{ m}^3/\text{m}^3$),
 613 whereas the rmse of the copula simulations was of $0.066 \text{ m}^3/\text{m}^3$
 614 (original LPRM rmse: $0.160 \text{ m}^3/\text{m}^3$).

615 LR is the site with the largest number of rain events, and as
 616 mentioned in the previous section, this high rain frequency was
 617 not properly captured during the fall season of 2010; this can
 618 be seen as well in the entire time series where all the copulas
 619 and CDF matching estimates were flat during fall seasons.
 620 Moreover, since SMOS was overestimating the soil moisture
 621 during the spring season of 2010, both statistical estimates had
 622 this behavior. Even though the tendency of the simulations was
 623 correct, the dynamic behavior was not well represented, which
 624 resulted in a very poor correlation coefficient (negative values
 625 in 2004 and 2007).

626 RC is a very complicated site because of the frequent
 627 snow and frozen soil events occurring during half of the year.
 628 However, statistical results were improved for the entire year

with copula simulations (rmse = $0.099 \text{ m}^3/\text{m}^3$ for LPRM and
 629 rmse = $0.056/0.062 \text{ m}^3/\text{m}^3$ for copulas/CDF matching). 630

VI. CONCLUSION AND PERSPECTIVES 631

The main goal of this study was to propose a new method to 632
 generate a long homogeneous time series (2003–2010) of soil 633
 moisture from two overlapping time series. 634

For that purpose, two statistical tools, the CDF matching and 635
 the copulas, were tested over four watersheds in the U.S. By 636
 using CDF matching, the assumption that the two studied data sets 637
 are ranked in the same way is made, which the copulas do not 638
 require. The two analyzed data sets (SMOS and LPRM) were 639
 jointly available only for 2010, so data from 2010 were used to 640
 estimate the CDFs that are used as references to estimate SMOS 641
 soil moisture for previous years. The novelty of the approach is 642
 its application: establishing the statistical relationship between 643

TABLE V
 STATISTICAL RESULTS FROM THE COMPARISON BETWEEN THE SIMULATED TIME SERIES OF SOIL MOISTURE FROM 2003 TO 2010. ORIGINAL SOIL MOISTURE TIMES ARE REPRESENTED BY LPRM. THE BEST RESULTS ARE INDICATED IN BOLD, AND THE RMSE ARE IN m^3/m^3 . (a) WG. (b) LW. (c) LR. (d) RC

		(a)								
		2003	2004	2005	2006	2007	2008	2009	2010	Total
LPRM	R	0.070	0.76	0.82	0.66	0.81	0.68	0.65	0.79	0.73
	RMSE	0.129	0.141	0.146	0.133	0.147	0.138	0.129	0.139	0.138
Copula	R	0.62	0.55	0.82	0.64	0.81	0.75	0.76	0.79	0.69
	RMSE	0.059	0.059	0.059	0.060	0.054	0.053	0.060	0.043	0.057
CDF m.	R	0.73	0.62	0.88	0.72	0.89	0.75	0.79	0.82	0.74
	RMSE	0.070	0.074	0.071	0.073	0.067	0.067	0.077	0.054	0.071

		(b)								
		2003	2004	2005	2006	2007	2008	2009	2010	Total
LPRM	R	0.56	0.71	0.48	0.67	0.32	0.42	0.52	0.58	0.55
	RMSE	0.163	0.149	0.187	0.149	0.173	0.158	0.149	0.149	0.160
Copula	R	0.56	0.47	0.19	0.62	0.41	0.64	0.58	0.71	0.47
	RMSE	0.071	0.064	0.088	0.077	0.060	0.056	0.051	0.044	0.066
CDF m.	R	0.59	0.60	0.34	0.63	0.49	0.61	0.53	0.71	0.51
	RMSE	0.083	0.070	0.101	0.092	0.069	0.076	0.069	0.059	0.079

		(c)								
		2003	2004	2005	2006	2007	2008	2009	2010	Total
LPRM	R	0.51	0.60	0.46	0.75	0.64	0.70	0.49	0.65	0.58
	RMSE	0.171	0.148	0.181	0.185	0.180	0.166	0.187	0.178	0.174
Copula	R	0.54	-0.48	0.73	0.01	-0.14	0.20	0.43	0.51	0.19
	RMSE	0.042	0.079	0.036	0.069	0.081	0.054	0.047	0.045	0.059
CDF m.	R	0.68	-0.16	0.72	0.28	0.18	0.50	0.55	0.59	0.37
	RMSE	0.044	0.080	0.042	0.070	0.085	0.050	0.048	0.048	0.061

		(d)								
		2003	2004	2005	2006	2007	2008	2009	2010	Total
LPRM	R	0.78	0.76	0.74	0.80	0.84	0.69	0.78	0.73	0.77
	RMSE	0.093	0.085	0.110	0.099	0.102	0.106	0.099	0.099	0.099
Copula	R	0.53	0.78	0.70	0.68	0.72	0.75	0.72	0.80	0.69
	RMSE	0.065	0.045	0.065	0.060	0.051	0.047	0.052	0.059	0.056
CDF m.	R	0.42	0.69	0.65	0.63	0.70	0.65	0.71	0.70	0.63
	RMSE	0.073	0.051	0.070	0.063	0.055	0.056	0.056	0.067	0.062

644 AMSR-E and SMOS retrieved soil moisture values and using
 645 this relationship to estimate the *equivalent* SMOS value for the
 646 AMSR-E period prior to the SMOS launch.

647 The first analysis of these simulations over 2010 showed that
 648 the simulated data sets were very similar to the SMOS estimates
 649 and reproduced SMOS behavior accurately except over the LR
 650 watershed where numerous rain events occurred. This high
 651 rainfall frequency was interpreted statistically as noise, and
 652 hence, the simulations did not describe the soil moisture evolu-
 653 tion over this site very well. RC was also a very complicated site
 654 due to the local topography and seasonal climate conditions.
 655 Soil moisture derived from satellite observations was not able
 656 to accurately reproduce the dynamics as found in the *in situ*
 657 data, and as a result, the simulated soil moisture did not either.
 658 However, the total rmse for the simulated soil moisture from
 659 copulas was reduced by a factor of almost 2. The WG and
 660 LW sites were well represented by the simulations, and copulas
 661 improved the error by a factor of 3, whereas CDF matching
 662 improved the correlation.

663 The time series of soil moisture were estimated from 2003 to
 664 2010 and were compared to *in situ* measurements at all four
 665 watersheds. Since simulated soil moisture data in 2010 over
 666 the LR watershed had very little dynamic range, they remained
 667 the same for the entire time series and showed very poor
 668 statistical results. Even though the rmse values were improved

by a factor of 3, the total correlation was not good. For the
 three other sites, the correlation coefficient was a bit degraded
 compared to the original LPRM data, but the rmse was highly
 improved with copulas by a factor of 2 to 3. In general, CDF
 matching gave better results in terms of correlation, and copulas
 gave better results in terms of errors compared to the ground
 measurements.

As a more general conclusion, CDF matching gives good
 results but does not take into account the structure of the
 dependence between the two data sets, whereas the copulas
 allow to model this structure. Through the choice of the family
 and the parameter θ (which controls the width of the tail of the
 scatter), it is possible to model all kinds of structures, from the
 perfect dependence (CDF matching), right or left dependence,
 to complete independence. This is why copulas produce better
 results for the extreme values (very low and very high values)
 than CDF matching. Copulas can also estimate the uncertainty
 of the soil moisture simulations given the LPRM value and
 can be seen as a quality information in the simulation process.
 However, the copula method is time consuming. It is quick
 to choose the copula family and its associated parameter as
 it is based on a Bayesian approach; however, it is very time
 consuming to generate the 1000 simulations, particularly if the
 chosen copula does not have an analytic inversion form. In the
 latter case, 1000 equations need to be resolved numerically.

694 Nevertheless, these simulations represent an advantage since it
695 is possible to compute a mean and a standard deviation. The
696 limitations are the same for both methods and even for any
697 general statistical methods using a specific year as a reference:
698 Only the variable range of this particular year can be well
699 represented. Therefore, if an event in a previous year occurs
700 and is out of the range found in the specific year of reference
701 (such as drought or flood events), then that event will not be
702 well represented in the simulated results.

703 In order to improve this methodology, applying a moving
704 window of three months would provide more accurate results
705 instead of dividing the year into four seasons. This would also
706 avoid the artifacts and gaps generally noticed at the transition
707 between the seasons. Another solution would be to introduce
708 the time in the copulas, but the level of complexity in the copula
709 manipulation would increase as well.

710 In this paper, the attempt to build a homogeneous soil mois-
711 ture time series has been based on statistical methods only. Of
712 course, other methods exist to reconcile different sensor ac-
713 quisitions, and because SMOS and AMSR-E do not operate at
714 the same frequencies and not at the same crossing times, using
715 physical models to tackle these discrepancies is an alternative to
716 statistical methods. Moreover, matching observations acquired
717 at 130 am and 600 am can trigger some questions, particularly
718 regarding the precipitations that could occur in between. The
719 present study is a first step toward a unified and homogeneous
720 soil moisture time series, and mixing physical and statisti-
721 cal models to do so would be a breakthrough for climate
722 studies.

723 The next step of this study is to build a homogeneous time
724 series of soil moisture at the global scale. Hence, the results of
725 this study will be extended in the future to build a global map
726 of the copula family choice and to study if there exists any rela-
727 tionship between the chosen copulas and the soil characteristics
728 or land use data. This would allow us to derive soil moisture
729 time series from LPRM data within SMOS soil moisture range
730 over the entire globe.

731 ACKNOWLEDGMENT

732 The authors would like to thank the USDA research team for
733 providing the *in situ* data and D. Huard from McGill University
734 for the helpful inputs on the copula method. USDA is an Equal
735 Employment Opportunity employer.

736 REFERENCES

737 [1] "Implementation Plan for the Global Observing System for Climate
738 in Support of the UNFCCC," World Meteorological Org., Geneva,
739 Switzerland, Tech. Rep., 2010.
740 [2] M. Drusch, "Initializing numerical weather predictions models with satel-
741 lite derived surface soil moisture: Data assimilation experiments with
742 ECMWF's integrated forecast system and the TMI soil moisture data set,"
743 *J. Geophys. Res.*, vol. 113, no. D3, p. D03 102, Feb. 2007.
744 [3] H. Douville and F. Chauvin, "Relevance of soil moisture for seasonal cli-
745 mate predictions: A preliminary study," *Climate Dyn.*, vol. 16, no. 10/11,
746 pp. 719–736, Oct. 2000.
747 [4] Y. Kerr, P. Waldteufel, J. Wigneron, S. Delwart, F. Cabot, J. Boutin,
748 M. Escorihuela, J. Font, N. Reul, C. Gruhier, S. Juglea, M. Drinkwater,
749 A. Hahne, M. Martin-Neira, and S. Mecklenburg, "The SMOS mission:
750 New tool for monitoring key elements of the global water cycle," *Proc.*
751 *IEEE*, vol. 98, no. 5, pp. 666–687, May 2010.

[5] D. Entekhabi, E. Njoku, P. O'Neill, K. Kellogg, W. Crow, W. Edelstein, 752
J. Entin, S. Goodman, T. Jackson, J. Johnson, J. Kimball, J. Piepmeier, 753
R. Koster, N. Martin, K. McDonald, M. Moghaddam, S. Moran, 754
R. Reichle, J. Shi, M. Spencer, S. Thurman, L. Tsang, and J. Zyl, "The 755
soil moisture active passive (SMAP) mission," *Proc. IEEE*, vol. 98, no. 5, 756
pp. 704–716, May 2010.
[6] Y. Kerr, P. Waldteufel, J. Wigneron, J. Martinuzzi, J. Font, and M. Berger, 757
"Soil moisture retrieval from space: The soil moisture and ocean salinity 759
(SMOS) mission," *IEEE Trans. Geosci. Remote Sens.*, vol. 39, no. 8, 760
pp. 1729–1735, Aug. 2001.
[7] M. Owe, R. de Jeu, and J. Walker, "A methodology for surface soil 762
moisture and vegetation optical depth retrieval using the microwave pol- 763
arization difference index," *IEEE Trans. Geosci. Remote Sens.*, vol. 39, 764
no. 8, pp. 1643–1654, Aug. 2001.
[8] E. Njoku, T. Jackson, V. Lakshmi, T. Chan, and S. Nghiem, "Soil moisture 766
retrieval from AMSR-E," *IEEE Trans. Geosci. Remote Sens.*, vol. 41, 767
no. 2, pp. 215–229, Feb. 2003.
[9] L. Li, P. Gaiser, B. Gao, R. Bevilacqua, T. Jackson, E. Njoku, C. Rüdiger, 769
J. Calvet, and R. Bindlish, "Windsat global soil moisture retrieval and 770
validation," *IEEE Trans. Geosci. Remote Sens.*, vol. 48, no. 5, pp. 2224– 771
2241, May 2010.
[10] V. Naeimi, K. Scipal, Z. Bartalis, and S. H. W. Wagner, "An improved soil 773
moisture retrieval algorithm for ERS and METOP scatterometer observa- 774
tions," *IEEE Trans. Geosci. Remote Sens.*, vol. 47, no. 7, pp. 1999–2013, 775
Jul. 2009.
[11] L. Vincent, X. Zhang, B. Bonsal, and W. Hogg, "Homogenization of 777
daily temperatures over Canada," *J. Climate*, vol. 15, no. 11, pp. 1322– 778
1334, Jun. 2002.
[12] M. Begert, T. Schlegel, and W. Kirchhofer, "Homogeneous temperature 780
and precipitation series of Switzerland from 1864 to 2000," *Int. J. Clima- 781
tol.*, vol. 25, no. 1, pp. 65–80, Jan. 2005.
[13] G. Picard and M. Fily, "Surface melting observations in Antarctica by 783
microwave radiometers: Correcting 26-year time series from changes in 784
acquisition hours," *Remote Sens. Environ.*, vol. 104, no. 3, pp. 325–336, 785
Oct. 2006.
[14] R. Reichle and R. Koster, "Bias reduction in short records of satellite soil 787
moisture," *Geophys. Res. Lett.*, vol. 31, no. 19, p. L19 501, Oct. 2004. 788
[15] M. Choi and J. Jacobs, "Temporal variability corrections for advanced 789
microwave scanning radiometer E (AMSR-E) surface soil moisture: 790
Case study in little river region, Georgia, U.S.," *Sensors*, vol. 8, no. 4, 791
pp. 2617–2627, Apr. 2008.
[16] H. Li, J. Sheffield, and E. Wood, "Bias correction of monthly precipitation 793
and temperature fields from IPCC AR4 models using equidistant quantile 794
matching," *J. Geophys. Res., Atmosp.*, vol. 115, no. D10, p. D10 101, 795
May 2010.
[17] M. Drusch, E. Wood, and H. Gao, "Observation operators for the di- 797
rect assimilation of TRMM microwave imager retrieved soil moisture," 798
Geophys. Res. Lett., vol. 32, no. 15, p. L15 403, Aug. 2005. 799
[18] Y. Liu, A. van Dijk, R. de Jeu, and T. Holmes, "An analysis of spatiotem- 800
poral variations of soil and vegetation moisture from a 29-year satellite- 801
derived data set over mainland Australia," *Water Resour. Res.*, vol. 45, 802
no. 7, p. W07 405, Jul. 2009. 803
[19] Y. Liu, R. Parinussa, W. Dorigo, R. D. Jeu, W. Wagner, A. V. Dijk, 804
M. McCabe, and J. Evans, "Developing an improved soil moisture dataset 805
by blending passive and active microwave satellite-based retrievals," 806
Hydrol. Earth Syst. Sci., vol. 15, no. 2, pp. 425–436, Feb. 2011. 807
[20] V. Singh and W. Strupczewski, "Editorial," *J. Hydrol. Eng.*, vol. 12, no. 4, 808
p. 345, Jul. 2007. 809
[21] R. Nelsen, "An introduction to copulas," in *Springer Series in Statistics*. 810
New York, NY, USA: Springer-Verlag, 1998. 811
[22] P. Trivedi and D. Zimmer, *Copula Modeling: An Introduction for Practi- 812
tioners*, vol. 1, *Foundations and Trends in Econometrics*. Hanover, MA, 813
USA: Now Publ. Inc., 2005, pp. 1–111. 814
[23] C. Hafner and O. Reznikova, "Efficient estimation of a semiparametric 815
dynamic copula model," *Comput. Stat. Data Anal.*, vol. 54, no. 11, 816
pp. 2609–2627, Nov. 2010. 817
[24] C. Genest and A. Favre, "Everything you always wanted to know about 818
copula modeling but were afraid to ask," *J. Hydrol. Eng.*, vol. 12, no. 4, 819
pp. 347–368, Jul./Aug. 2007. 820
[25] A. Favre, S. E. Adlouni, L. Perreault, N. Thiémond, and B. Bobée, "Mul- 821
tivariate hydrological frequency analysis using copulas," *Water Resour.* 822
Res., vol. 40, no. 1, p. W01 101, Jan. 2004. 823
[26] G. Salvadori and C. de Michele, "On the use of copulas in hydrology: 824
Theory and practice," *J. Hydrol. Eng.*, vol. 12, no. 4, pp. 369–380, 825
Jul. 2007. 826
[27] D. Dupuis, "Using Copulas in hydrology: Benefits, cautions and issues," 827
J. Hydrol. Eng., vol. 12, no. 4, pp. 381–393, Jul. 2007. 828

829 [28] L. Zhang and V. Singh, "Trivariate flood frequency analysis using the
830 Gumbel-Hougaard copula," *J. Hydrol. Eng.*, vol. 12, no. 4, pp. 431–439,
831 Jul. 2007.

832 [29] F. Serinaldi and S. Grimaldi, "Fully nested 3-copula: Procedure and appli-
833 cation on hydrological data," *J. Hydrol. Eng.*, vol. 12, no. 4, pp. 420–430,
834 Jul. 2007.

835 [30] P. Laux, S. Vogl, W. Qiu, H. Knoche, and H. Kunstmann, "Copula-based
836 statistical refinement of precipitation in RCM simulations over complex
837 terrain," *Hydrol. Earth Syst. Sci.*, vol. 15, no. 7, pp. 2401–2419, Jul. 2011.

838 [31] H. Gao, E. Wood, M. Drusch, and M. McCabe, "Copula-derived observa-
839 tion operators for assimilating TMI and AMSR-E retrieved soil moisture
840 into land surface models," *J. Hydrometeorol.*, vol. 8, no. 3, pp. 413–429,
841 Jun. 2007.

842 [32] C. de Michele and G. Salvadori, "A generalized pareto intensity-duration
843 model of storm rainfall exploiting 2-copulas," *J. Geophys. Res.*, vol. 108,
844 no. D2, p. 4067, Jan. 2003.

845 [33] J. Wigneron, Y. Kerr, P. Waldteufel, K. Saleh, M. Escorihuela,
846 P. Richaume, P. Ferrazzoli, P. de Rosnay, R. Gurney, J. Calvet, J. Grant,
847 M. Guglielmetti, B. Hornbuckle, C. Mätzler, T. Pellarin, and M. Schwank,
848 "L-band microwave emission of the biosphere (L-MEB) model: Descrip-
849 tion and calibration against experimental data sets over crop fields,"
850 *Remote Sens. Environ.*, vol. 107, no. 4, pp. 639–655, Apr. 2007.

851 [34] Y. Kerr, P. Waldteufel, P. Richaume, J. Wigneron, P. Ferrazzoli,
852 A. Mahmoodi, A. A. Bitar, F. Cabot, C. Gruhier, S. Juglea, D. Leroux,
853 A. Mialon, and S. Delwart, "The SMOS soil moisture retrieval algo-
854 rithm," *IEEE Trans. Geosci. Remote Sens.*, vol. 50, no. 5, pp. 1384–1403,
855 May 2012.

856 [35] D. Carr, R. Kahn, K. Sahr, and T. Olsen, "ISEA discrete global grids,"
857 *Stat. Comput. Stat. Graph. Newl.*, vol. 8, no. 2/3, pp. 31–39, 1997.

858 [36] A. A. Bitar, D. Leroux, Y. Kerr, O. Merlin, P. Richaume, A. Sahoo, and
859 E. Wood, "Evaluation of SMOS soil moisture products over continental
860 US using SCAN/SNOTEL network," *IEEE Trans. Geosci. Remote Sens.*,
861 vol. 50, no. 5, pp. 1572–1586, May 2012.

862 [37] G. Schaefer, M. Cosh, and T. Jackson, "The USDA natural resources
863 conservation service soil climate analysis network (SCAN)," *J. Atmosf.*
864 *Ocean. Technol.*, vol. 24, no. 12, pp. 2073–2077, Dec. 2007.

865 [38] T. Jackson, R. Bindlish, M. Cosh, T. Zhao, P. Starks, D. Bosch,
866 M. Seyfried, S. Moran, Y. Kerr, and D. Leroux, "Validation of soil mois-
867 ture and ocean salinity (SMOS) soil moisture over watershed networks in
868 the U.S.," *IEEE Trans. Geosci. Remote Sens.*, vol. 50, no. 5, pp. 1530–
869 1543, May 2012.

870 [39] D. Leroux, Y. Kerr, A. A. Bitar, C. Gruhier, R. Bindlish, T. Jackson,
871 B. Berthelot, and G. Portet, "Comparison between SMOS, VUA, ASCAT
872 and ECMWF soil moisture products over four watersheds in the U.S.,"
873 *IEEE Trans. Geosci. Remote Sens.*, submitted for publication.

874 [40] J. Sabatier, A. Fouilloux, and P. de Rosnay, "Technical implementation
875 of SMOS data in the ECMWF integrated forecast system," *IEEE Geosci.*
876 *Remote Sens. Lett.*, vol. 9, no. 2, pp. 252–256, Mar. 2012.

877 [41] [Online]. Available: <ftp://n4ftl01u.ecs.nasa.gov/SAN/AMSA/>

878 [42] C. Gruhier, P. de Rosnay, Y. Kerr, E. Ceschia, J. Calvet, and
879 P. Richaume, "Evaluation of AMSR-E soil moisture product based on
880 ground measurements over temperate and semi-arid regions," *Geophys.*
881 *Res. Lett.*, vol. 35, no. 10, p. L10 405, May 2008.

882 [43] C. Rudiger, J. C. Calvet, C. Gruhier, T. Holmes, R. de Jeu, and
883 W. Wagner, "An intercomparison of ERS-SCAT and AMSR-E soil mois-
884 ture observations with model simulations over France," *Amer. Meteorol.*
885 *Soc.*, vol. 10, no. 2, pp. 431–447, Apr. 2009.

886 [44] C. Draper, J. Walker, P. Steinle, R. de Jeu, and T. Holmes, "An evaluation
887 of AMSR-E derived soil moisture over Australia," *Remote Sens. Environ.*,
888 vol. 113, no. 4, pp. 703–710, Apr. 2009.

889 [45] C. Gruhier, P. de Rosnay, S. Hasenauer, T. Holmes, R. de Jeu, Y. Kerr,
890 E. Mougou, E. Njoku, F. Timouk, W. Wagner, and M. Zribi, "Soil moisture
891 active and passive microwave products: Intercomparison and evaluation
892 over a Sahelian site," *Hydrol. Earth Syst. Sci.*, vol. 14, no. 1, pp. 141–156,
893 Jan. 2010.

894 [46] S. Chaurasia, D. Tung, P. Thapliyal, and P. Joshi, "Assessment of AMSR-
895 E soil moisture product over India," *Int. J. Remote Sens.*, vol. 32, no. 23,
896 pp. 7955–7970, Dec. 2011.

897 [47] T. Jackson, M. Cosh, R. Bindlish, P. Starks, D. Bosch, M. Seyfried,
898 D. Goodrich, M. Moran, and J. Du, "Validation of advanced microwave
899 scanning radiometer soil moisture products," *IEEE Trans. Geosci. Remote*
900 *Sens.*, vol. 48, no. 12, pp. 4256–4272, Dec. 2010.

901 [48] B. Schweizer and E. Wolff, "On nonparametric measures of dependence
902 for random variables," *Ann. Stat.*, vol. 9, no. 4, pp. 879–885, Jul. 1981.

903 [49] Y. Wang and H. Pham, "Modeling the dependent competing risks with
904 multiple degradation processes and random shock using time-varying
905 copulas," *IEEE Trans. Rel.*, vol. 61, no. 1, pp. 13–22, Mar. 2012.

[50] C. Genest and L.-P. Rivest, "Statistical inference procedures for bivariate
906 Archimedean copulas," *J. Amer. Stat. Assoc.*, vol. 88, no. 423, pp. 1034–
907 1043, Sep. 1993.

[51] J. Fermanian, "Goodness of fit tests for copulas," *J. Multivariate Anal.*,
909 vol. 95, no. 1, pp. 119–152, Jul. 2005.

[52] C. Genest, J.-F. Quessy, and B. Rémillard, "Goodness-of-fit procedures
911 for copula models based on the probability integral transform," *Scand. J.*
912 *Stat.*, vol. 33, no. 2, pp. 337–366, Jun. 2006.

[53] C. Genest and B. Rémillard, "Validity of the parametric bootstrap
914 for goodness-of-fit testing in semiparametric models," *Annales Henri*
915 *Poincaré*, vol. 44, no. 6, pp. 1096–1127, 2008.

[54] D. Berg, "Copula goodness-of-fit testing: An overview and power com-
917 parison," *Eur. J. Finance*, vol. 15, no. 7/8, pp. 675–701, 2009.

[55] C. Genest, B. Rémillard, and D. Beaudoin, "Goodness-of-fit tests for
919 copulas: A review and a power study," *Insurance: Math. Econom.*, vol. 44,
920 no. 2, pp. 199–213, Apr. 2009.

[56] D. Huard, G. Evin, and A. Favre, "Bayesian copula selection," *Comput.*
922 *Stat. Data Anal.*, vol. 51, no. 2, pp. 809–822, Nov. 2006.



Delphine J. Leroux received the M.S. degree in 924
applied mathematics from Institut National des Sci- 925
ences Appliquées, Toulouse, France, in 2009 and the 926
Ph.D. degree in spatial hydrology from Université 927
Paul Sabatier, Toulouse, in 2012. 928

From 2009 to 2012, she was with the Centre 929
d'Etudes Spatiales de la Biosphère, Toulouse, where 930
she worked on the validation of the Soil Moisture 931
and Ocean Salinity soil moisture product at the local 932
and global scales by using statistical and physical 933
methods. She is currently with the Jet Propulsion 934

Laboratory (JPL), Pasadena, CA, USA, on the Soil Moisture Active Passive 935
mission. 936

AQ28



Yann H. Kerr (M'88–SM'01–F'13) received the 937
engineering degree from Ecole Nationale Supérieure 938
de l'Aéronautique et de l'Espace, Toulouse, France, 939
the M.Sc. degree in electronics and electrical engi- 940
neering from Glasgow University, Glasgow, U.K., 941
and the Ph.D. degree in astrophysique géophysique 942
et techniques spatiales from Université Paul Sabatier, 943
Toulouse. 944

He is currently the Director of the Centre d'Etudes 945
Spatiales de la Biosphère, Toulouse. His fields of 946
interest are in the theory and techniques for mi- 947

crowave and thermal infrared remote sensing of the Earth, with emphasis 948
on hydrology and water resource management. He was an EOS Principal 949
Investigator (interdisciplinary investigations) and PI and precursor of the use 950
of the SCAT over land. In 1990, he started to work on the interferometric 951
concept applied to passive microwave Earth observation and was subsequently 952
the Science Lead on the MIRAS project for ESA. In 1997, he proposed the 953
Soil Moisture and Ocean Salinity (SMOS) mission, the natural outcome of the 954
previous MIRAS work. He is currently involved in the exploitation of SMOS 955
data, in the Cal Val activities and related level 2 soil moisture and level 3 and 4 956
developments. He is also working on the SMOS next concept. 957

Dr. Kerr received the World Meteorological Organization 1st prize (Norbert 958
Gerber), the USDA Secretary's team award for excellence (Salsa Program), 959
and the GRSS certificate of recognition for leadership in the development of 960
the first synthetic aperture microwave radiometer in space and success of the 961
SMOS mission and is a Distinguished Lecturer for GRSS. 962

AQ30
AQ31
AQ32
AQ33

AQ34
AQ35

AQ36

AQ37

AQ38

AQ39

AQ27



Eric F. Wood received the B.A.Sc. degree in civil engineering from the University of British Columbia, Vancouver, BC, Canada, in 1970 and the S.M., C.E., and Sc.D. degrees in civil engineering from the Massachusetts Institute of Technology, Cambridge, MA, USA, in 1972, 1973, and 1974, respectively.

He is currently a Professor in the Department of Civil and Environmental Engineering, Princeton University, NJ, USA. His recent contributions include the macroscale hydrologic prediction of the coupled water and energy balances of the land surface, remote sensing as an integral tool for observation and modeling of the hydrologic cycle, and developing and evaluating seasonal hydrological forecasts based on coupled seasonal climate forecasts.

Dr. Wood is a fellow of the American Geophysical Union and the American Meteorological Society. He received, among other honors, the Robert E. Horton Award from the Hydrology Section of the American Geophysical Union (1977), the John Dalton Medal from the European Geophysical Union (2007), and the Jules G. Charney Award from the American Meteorological Society (2010).



Alok K. Sahoo received the Ph.D. degree in computational sciences from George Mason University, Fairfax, VA, USA, in 2008.

After finishing his Ph.D., he worked as a Research Associate at the Institute of Global Environment and Society, Beltsville, MD, USA, from 2008 to 2009. He is currently an Associate Research Hydrologist with the Department of Civil and Environmental Engineering, Princeton University, Princeton, NJ, USA. His research interests involve the application of microwave remote sensing in hydrologic applications.

His current research projects include soil moisture estimation from microwave sensors and checking consistency among hydrologic cycle variables for drought monitoring.



Rajat Bindlish (S'98-AM'99-M'03-SM'05) received the B.S. degree in civil engineering from the Indian Institute of Technology, Bombay in 1993 and the M.S. and Ph.D. degrees in civil engineering from The Pennsylvania State University in 1996 and 2000, respectively.

He is currently with SSAI, working at USDA Agricultural Research Service, Hydrology and Remote Sensing Laboratory, Beltsville, MD, USA. His research interests involve the application of microwave remote sensing in hydrology. He is currently working on soil moisture estimation from microwave sensors and their subsequent application in land surface hydrology.



Thomas J. Jackson (SM'96-F'02) received the Ph.D. degree from the University of Maryland, College Park, MD, USA, in 1976.

He is a Research Hydrologist with the U.S. Department of Agriculture, Agricultural Research Service, Hydrology and Remote Sensing Laboratory, Beltsville, MD, USA. His research involves the application and development of remote sensing technology in hydrology and agriculture, primarily the microwave measurement of soil moisture.

Dr. Jackson is or has been a member of the science and validation teams of the Aqua, ADEOS-II, Radarsat, Oceansat-1, Envisat, ALOS, Soil Moisture and Ocean Salinity, Aquarius, GCOM-W, and Soil Moisture Active Passive remote sensing satellites. He is a fellow of the Society of Photo-Optical Instrumentation Engineers, the American Meteorological Society, and the American Geophysical Union. In 2003, he received the William T. Pecora Award (NASA and Department of Interior) for outstanding contributions toward understanding the Earth by means of remote sensing and the AGU Hydrologic Sciences Award for outstanding contributions to the science of hydrology. He received the IEEE Geoscience and Remote Sensing Society Distinguished Achievement Award in 2011.

AUTHOR QUERIES

AUTHOR PLEASE ANSWER ALL QUERIES

Please be aware that the authors are required to pay overlength page charges (\$200 per page) if the paper is longer than 6 pages. If you cannot pay any or all of these charges please let us know.

This pdf contains 2 proofs. The first half is the version that will appear on Xplore. The second half is the version that will appear in print. If you have any figures to print in color, they will be in color in both proofs.

- AQ1 = The sentence was restructured for clarity. Please check if the original thought was retained, and correct if necessary.
- AQ2 = Please provide the expanded form of “USDA.”
- AQ3 = Please provide the expanded form of “ARS.”
- AQ4 = The sentence was restructured for clarity. Please check if the original thought was retained, and correct if necessary.
- AQ5 = The sentence was restructured for clarity. Please check if the original thought was retained, and correct if necessary.
- AQ6 = “AMSR-E” is defined as “Advanced Microwave Scanning Radiometer-Earth Observing System” for consistency. Please check if appropriate, and correct if necessary.
- AQ7 = The sentence was restructured for clarity. Please check if the original thought was retained, and correct if necessary.
- AQ8 = “Picard *et al.*” was changed to “Picard and Fily.” Please check if appropriate, and correct if necessary.”
- AQ9 = The sentence was rephrased for clarity. Please check if the original thought was retained, and correct if necessary.
- AQ10 = The sentence was rephrased for clarity. Please check if the original thought was retained, and correct if necessary.
- AQ11 = The sentence was rephrased for clarity. Please check if the original thought was retained, and correct if necessary.
- AQ12 = The sentence was restructured for clarity. Please check if the original thought was retained, and correct if necessary.
- AQ13 = “rmse” is defined as “root-mean-square error.” Please check if appropriate, and correct if necessary.”
- AQ14 = The sentence was rephrased. Please check if the original thought was retained, and correct if necessary.”
- AQ15 = Please provide the expanded form of “NASA.”
- AQ16 = The sentence was rephrased for clarity. Please check if the original thought was retained, and correct if necessary.
- AQ17 = The sentence was rephrased for clarity. Please check if the original thought was retained, and correct if necessary.
- AQ18 = The caption was rephrased for clarity. Please check if the original thought was retained, and correct if necessary.
- AQ19 = The sentence was rephrased for clarity. Please check if the original thought was retained, and correct if necessary.
- AQ20 = “CDF” is defined as “cumulative density function” for consistency. Please check if appropriate, and correct if necessary.
- AQ21 = The sentence was rephrased for clarity. Please check if the original thought was retained, and correct if necessary.

- AQ22 = The sentence was rephrased for clarity. Please check if the original thought was retained, and correct if necessary.
- AQ23 = The sentence was rephrased for clarity. Please check if the original thought was retained, and correct if necessary.
- AQ24 = The sentence was rephrased for clarity. Please check if the original thought was retained, and correct if necessary.
- AQ25 = The sentence was rephrased for clarity. Please check if the original thought was retained, and correct if necessary.
- AQ26 = The sentence was rephrased for clarity. Please check if the original thought was retained, and correct if necessary.
- AQ27 = Please provide publication update in Ref. [39].
- AQ28 = The author's current affiliation indicated in the footnote did not correspond to the current affiliation provided in the curriculum vitae. Please check.
- AQ29 = The sentence was rephrased for clarity. Please check if the original thought was retained, and correct if necessary.
- AQ30 = The sentence was rephrased for clarity. Please check if the original thought was retained, and correct if necessary.
- AQ31 = Please provide the expanded form of "EOS."
- AQ32 = Please provide the expanded form of "PI."
- AQ33 = Please provide the expanded form of "SCAT."
- AQ34 = Please provide the expanded form of "MIRAS."
- AQ35 = Please provide the expanded form of "ESA."
- AQ36 = Please provide the expanded form of "Cal Val."
- AQ37 = "Dr." was inserted as the title for author Yann H. Kerr. Please check if appropriate, and correct if necessary.
- AQ38 = Please provide the expanded form of "GRSS."
- AQ39 = The sentence was rephrased for clarity. Please check if the original thought was retained, and correct if necessary.
- AQ40 = Please provide the specific location of the Indian Institute of Technology, Bombay.
- AQ41 = Please provide the specific location of The Pennsylvania State University.
- AQ42 = Please provide the expanded form of "SSAI."
- AQ43 = Please provide the expanded form of "ADEOS-II."
- AQ44 = Please provide the expanded form of "ALOS."
- AQ45 = Please provide the expanded form of "GCOM-W."
- AQ46 = Please provide the expanded form of "AGU."

END OF ALL QUERIES

1 An Approach to Constructing a Homogeneous Time 2 Series of Soil Moisture Using SMOS

3 Delphine J. Leroux, Yann H. Kerr, *Fellow, IEEE*, Eric F. Wood, Alok K. Sahoo,
4 Rajat Bindlish, *Senior Member, IEEE*, and Thomas J. Jackson, *Fellow, IEEE*

5 **Abstract**—Overlapping soil moisture time series derived
6 from two satellite microwave radiometers (the Soil Moisture
7 and Ocean Salinity and the Advanced Microwave Scanning
8 Radiometer-Earth Observing System) are used to generate a soil
9 moisture time series from 2003 to 2010. Two statistical methodolo-
10 gies for generating long homogeneous time series of soil moisture
11 are considered. Generated soil moisture time series using only
12 morning satellite overpasses are compared to ground measure-
13 ments from four watersheds in the U.S.A. with different clima-
14 tologies. The two methods, cumulative density function (CDF)
15 matching and copulas, are based on the same statistical theory, but
16 the first makes the assumption that the two data sets are ordered
17 the same way, which is not needed by the second. Both methods
18 are calibrated in 2010, and the calibrated parameters are applied
19 to the soil moisture data from 2003 to 2009. Results from these
20 two methods compare well with ground measurements. However,
21 CDF matching improves the correlation, whereas copulas improve
22 the root-mean-square error.

23 **Index Terms**—Advanced Microwave Scanning Radiometer-
24 Earth Observing System (AMSR-E), cumulative density func-
25 tion (CDF) matching, copulas, Soil Moisture and Ocean Salinity
26 (SMOS), soil moisture, time series.

27 I. INTRODUCTION

28 **S**OIL moisture is an important variable and is now consid-
29 ered as an essential climate variable by the World Meteoro-
30 logical Organization [1]. It has a crucial role in the transfers
31 of water and energy between the soil and the atmosphere. Soil
32 moisture is also an input variable for land surface modeling
33 in determining the evaporative fraction at the surface and the
34 infiltration in the root zone. For both agriculture and water
35 resource management, soil moisture information is essential at
36 local and regional scales. At global scales, soil moisture is of

great value for weather forecasting [2], climate change [3], and
37 monitoring extreme events such as floods and droughts. 38

Soil Moisture and Ocean Salinity (SMOS) [4] was success-
39 fully launched by the European Space Agency in November 40
2009 and since has been providing global maps of soil moisture 41
every three days at a nominal spatial resolution of 43 km 42
with an accuracy of $0.04 \text{ m}^3/\text{m}^3$. SMOS is the first mission 43
specifically designed for soil moisture monitoring. The Soil 44
Moisture Active Passive (SMAP) mission [5] is scheduled 45
for launch in October 2014 by the National Aeronautics and 46
Space Administration. SMAP will continue the time series of 47
soil moisture based on 1.4-GHz radiometer observations that 48
began with SMOS. The 1.4-GHz frequency channel is the most 49
suitable frequency for soil moisture retrieval [6]. 50

Longer time series of satellite-based soil moisture would be 51
of value in climate-related analysis. Utilizing the data from the 52
previous generations of satellite sensors involves resolving nu- 53
merous issues. Some of the platforms and approaches have been 54
developed to retrieve soil moisture using the higher frequencies, 55
which has been the only option until now. These include the 56
Scanning Multichannel Microwave Radiometer (1978–1987) 57
[7], the Special Sensor Microwave/Imager (1987–current) 58
[7], the Advanced Microwave Scanning Radiometer-Earth 59
Observing System (AMSR-E) (2002–2011) [7], [8], Wind- 60
Sat (2003–current) [9], and the European Remote Sensing- 61
Advanced Scatterometer (1991–current) [10]. Although their 62
lowest frequencies (5–20 GHz) are not the most suitable for 63
soil moisture retrievals (higher sensitivity to vegetation growth 64
and atmospheric conditions), they remain a valuable time series 65
from 1978 until now. Applications such as data assimilation 66
or climate change assessment require consistent products. The 67
products referenced earlier have been retrieved using different 68
sensors with different algorithms, and as a result, the time series 69
is not homogeneous. This heterogeneity can be interpreted as a 70
bias and is a problem in the data assimilation process. To avoid 71
this issue, these products need to be processed to correct for any 72
bias or amplitude variation between the data sets. 73

Many previous studies have developed various methods for 74
the homogenization of time series. Vincent *et al.* [11] developed 75
a method to harmonize temperature time series with gaps. The 76
first step was to determine if the series was homogeneous by 77
comparing its anomalies to those of a reference series. The 78
identification of the gaps and their magnitude was performed 79
by successively fitting a linear model with different magnitude 80
values with the best fit being indicated by the minimum sum 81
of square errors. Homogeneous temperature and precipitation 82
time series were developed by Begert *et al.* [12] using statistical 83

Manuscript received November 28, 2011; revised May 14, 2012 and
October 22, 2012; accepted December 22, 2012. This work was supported in
part by Telespazio France and in part by TOSCA.

D. J. Leroux is with the Centre d'Etudes Spatiales de la Biosphere, 31400
Toulouse, France, and also with Telespazio France, 31023 Toulouse Cedex 1,
France (e-mail: delphine.j.leroux@gmail.com).

Y. H. Kerr is with the Centre d'Etudes Spatiales de la Biosphere, 31400
Toulouse, France (e-mail: yann.kerr@cesbio.cnes.fr).

E. F. Wood and A. K. Sahoo are with the Department of Civil and Environ-
mental Engineering, Princeton University, Princeton, NJ 08544 USA (e-mail:
efwood@princeton.edu; aksahoo2004@gmail.com).

R. Bindlish and T. J. Jackson are with the USDA ARS Hydrology and Re-
mote Sensing Laboratory, Beltsville, MD 20705 USA (e-mail: rajat.bindlish@
ars.usda.gov; tom.jackson@ars.usda.gov).

Color versions of one or more of the figures in this paper are available online
at <http://ieeexplore.ieee.org>.

Digital Object Identifier 10.1109/TGRS.2013.2240691

84 methods to detect potential inhomogeneity. In that study, a
 85 reference time series was necessary in order to detect and
 86 compute the magnitude of the shifts. Picard and Fily [13]
 87 proposed a method to simulate a homogeneous time series of
 88 the cumulative melting surface in Antarctica. Using satellite
 89 observations from different sensors and acquisition times was
 90 the biggest challenge. Correcting for the effect of the observing
 91 time was accomplished in two steps. First, a sinusoidal function
 92 with a 24-h periodicity was fitted, and then, an optimal interpo-
 93 lation to refine this first guess model to *force* it to be closer was
 94 applied to the observations and to provide very low uncertainty
 95 around observation time and larger uncertainty when there is no
 96 available observation.

97 Matching the cumulative density functions (CDFs) of two
 98 data sets has been used in several studies to merge time series.
 99 Reichle and Koster [14] and Choi and Jacobs [15] merged
 100 soil moisture derived from satellite observations with model
 101 data, and Li *et al.* [16] corrected the bias of precipitation
 102 and temperature products derived from different models. CDF
 103 matching was also used as a preliminary step of the assimilation
 104 process [17] and to produce long time series of soil moisture
 105 [18], [19].

106 Over the last few years, a new method based on copula
 107 functions has been developed. It allows the derivation of bi-
 108 variate distributions without making the assumptions required
 109 when dealing with multivariate frequency distributions, e.g.,
 110 the same type of marginal distribution for both variables, a
 111 joint normal distribution, and independent variables. One of
 112 the major advantages of the copula method is that the marginal
 113 distributions can be of any form [20]. The first comprehensive
 114 treatment of copulas was by Nelsen [21]. He presented methods
 115 to construct copulas and discussed the role played by copulas
 116 in modeling and dependence. Since then, copulas have been
 117 applied in various applications with the majority of the liter-
 118 ature dedicated to the financial sector [22], [23]. In the field of
 119 hydrology, some applications have emerged. Genest and Favre
 120 [24] summarized the existing methods to detect and evaluate
 121 the dependence between the data sets through copulas (analyt-
 122 ically and graphically) and enumerated the various methods to
 123 choose the best copula family and estimate their parameters.
 124 Favre *et al.* [25] applied copulas to peak flows and volumes
 125 from two watersheds, Salvadori and De Michele [26] to storm
 126 and rainfall time series, Dupuis [27] to the volume and duration
 127 of low flows of two rivers, Zhang and Singh [28] to rainfall fre-
 128 quency, Serinaldi and Grimaldi [29] to flood and sea frequency,
 129 and Laux *et al.* [30] to precipitation data. Gao *et al.* [31] used
 130 copulas as a preprocessing step for the assimilation process on
 131 soil moisture data.

132 Joint statistical analysis has already been applied when the
 133 sources of the soil moisture measurements come from different
 134 observation systems (e.g., AMSR-E surface soil moisture and
 135 10-cm soil moisture from a land surface model [14]). Similarly,
 136 joint statistical methods form the basis for data assimilation of
 137 satellite soil moisture into land surface models [31]. There are
 138 many other studies related to joint probability, including where
 139 the variables are physically different but where their statistical
 140 relationships are useful (e.g., rainfall storm intensity and storm
 141 duration [32]).

The goal of this paper is to estimate for all the AMSR-E 142
 period (2003–2010) SMOS-equivalent observations that can be 143
 used to develop a statistical representation of SMOS retrieval so 144
 that current and future SMOS retrievals can be used in applica- 145
 tions like drought monitoring based on percentiles. However, 146
 matching 130 am C-/X-band (AMSR-E) observations with 147
 600 am L-band (SMOS) observations presents some issues: 148
 1) The crossing times are different, and rainfalls may occur be- 149
 tween the two acquisitions; and 2) the frequencies are different, 150
 so the sensing depths are not similar. 151

The statistical impact of the rainfalls that could occur be- 152
 tween 130 am and 600 am is to lower the correlation. However, 153
 if the correlation is sufficiently high, a statistical relationship 154
 can be established to estimate an equivalent SMOS value from 155
 an AMSR-E observation. This high correlation implies that the 156
 occurrence of precipitation between the SMOS and AMSR-E 157
 overpasses is rare. Moreover, it is well known that soil moisture 158
 has a long temporal correlation time scale, so the overpass time 159
 differences will have a minimal effect on the analysis. 160

The impact of the different frequencies between AMSR-E 161
 and SMOS is, in most situations, not significant. The higher 162
 AMSR-E frequency (10.7 GHz) results in a more superficial 163
 emission depth than the SMOS observations, so while the 164
 retrieved values may be different, their relative values will be 165
 similar (both dry or wet). The correlation between paired ob- 166
 servations depends on their relative values (with their individual 167
 time series) and not absolute values, and in the case of copula- 168
 based joint distributions, the correlation is represented by the 169
 Kendall tau whose calculation is based on ranks. 170

If the two sensing depths were to be reconciled physically, 171
 given the soil property variability (spatially and with depth) 172
 with different wetting and drying properties, a physical model 173
 would introduce significant uncertainty that could be very 174
 difficult to estimate afterward. If the SMOS (or AMSR-E) 175
 data were adjusted to the AMSR-E (or SMOS) emission depth 176
 through data assimilation into a land surface model for exam- 177
 ple, then the complete record would have to be adjusted with 178
 the added uncertainty of the data assimilation step. With any 179
 of the suggested adjustments, there is a mismatch with the 180
 past or with the future. Only by treating the original data sets 181
 and determining the information content between them can a 182
 consistent approach be represented. 183

Data assimilation could, however, deal with the precipitation 184
 and the difference in sensing depth issues, but that would imply 185
 other uncertainties such as the space–time variability of the 186
 precipitation data sets, as well as other meteorological issues. 187
 Building a homogeneous time series based on data assimila- 188
 tion into a land surface model can be seen as a competing 189
 approach. 190

In this paper, we show two statistical methods to obtain 191
 this homogeneous time series. The satellite data and the four 192
 watersheds where the time series are simulated are presented 193
 in Section II. The two statistical methods for generating ho- 194
 mogeneous time series are presented in Section III which 195
 includes the general theory and how to apply them to real data. 196
 Simulated time series over the four watersheds are presented in 197
 Section IV. Conclusions and perspectives are described in the 198
 last section. 199

200 II. REGIONS OF INTEREST AND SATELLITE DATA

201 A. SMOS

202 With its L-band radiometer, SMOS [4] has been providing
 203 soil moisture data for almost three years and global coverage
 204 every three days with a 43-km resolution. The satellite is polar
 205 orbiting with equator crossing times of 6 am (local solar time
 206 (LST), ascending) and 6 pm (LST, descending). The signal at
 207 L-band is mainly influenced by the water content at the surface
 208 of the soil (around 5 cm).

209 SMOS acquires brightness temperatures at multiple inci-
 210 dence angles, from 0° to 55° with full polarization. The an-
 211 gular signature is a key element of the retrieval algorithm
 212 that provides soil moisture and the vegetation optical thickness
 213 through the minimization of a cost function between modeled
 214 and acquired brightness temperatures [33], [34]. This estimated
 215 soil moisture is referred as the Level 2 product [34] and is
 216 available on the Icosahedral Snyder Equal Area-4h9 grid [35].
 217 The nodes of this grid are equally spaced at about 15 km. In
 218 this paper, the 2010 SMOS Level 2 version 4 products have
 219 been used.

220 Currently, numerous studies are underway on the validation
 221 of SMOS soil moisture product with *in situ* measurements
 222 and estimates of other sensors and models. Bitar *et al.* [36]
 223 used the Soil Climate Analysis Network [37] and the Snow-
 224 pack Telemetry sites in North America to compare SMOS
 225 soil moisture retrievals and ground measurements. That study
 226 showed that SMOS soil moisture had a very good dynamic
 227 response but tended to underestimate the values. However,
 228 the new version of the product (V4) significantly improved
 229 the general results. Jackson *et al.* [38] studied SMOS soil
 230 moisture and vegetation optical depth over four watersheds in
 231 the U.S. They concluded that SMOS almost met the accuracy
 232 requirement with root-mean-square errors (rmse) of 0.043 and
 233 0.047 m³/m³ in the morning and afternoon, respectively,
 234 whereas the vegetation optical depth retrievals were not reliable
 235 yet for use in vegetation analyses. Leroux *et al.* [39] compared
 236 SMOS data with other satellite and model output products over
 237 the same four watersheds for the year 2010. It showed that
 238 SMOS soil moisture data were closer to the ground measure-
 239 ments than the other data sets. Even though the correlation
 240 coefficient was not the best, the bias was extremely small.

241 After the results of the validation activities, the European
 242 Center for Medium-Range Weather Forecasts has decided and
 243 is now ready to process SMOS data in near real time into their
 244 Integrated Forecast System. It is expected to have an impact on
 245 the weather forecast at short and medium ranges [40].

246 B. AMSR-E

247 The AMSR-E was launched in June 2002 on the Aqua
 248 satellite. This radiometer acquires data with a single 55° inci-
 249 dence angle at six different frequencies: 6.9, 10.7, 18.7, 23.8,
 250 36.5, and 89.0 GHz, all dual polarized. The crossing times are
 251 respectively 1:30 am (LST, descending) and 1:30 pm (LST,
 252 ascending).

253 There are several soil moisture products available that are
 254 based on AMSR-E data. Many studies have already showed

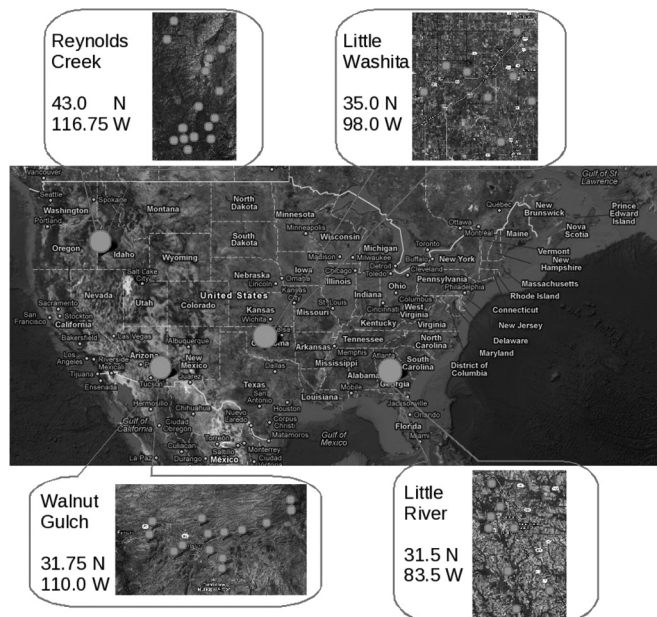


Fig. 1. Map of the four sites: WG, AZ; LW, OK; LR, GA; and RC, ID.

that the NASA product [41] is not able to reproduce low values
 of soil moisture and has low dynamic range [42]–[46]. The
 soil moisture data produced by the joint collaboration of the
 Vrije University of Amsterdam and NASA (whereafter called
 the Land Parameter Retrieval Model (LPRM) [7]) were chosen
 in this study.

The LPRM [7] retrieves soil moisture and optical thickness
 using the C- and X-band AMSR-E channels (combined prod-
 uct) and 36.5 GHz to estimate the surface temperature. This
 algorithm is based on a microwave radiative transfer model with
a priori information about soil characteristics. The products are
 available on a 0.25° × 0.25° grid only for the descending orbit.
 These data have been quality controlled, and the contaminated
 estimates due to high topography and extreme weather condi-
 tions such as snow have been flagged and not been considered
 in this study.

C. Study Areas

Four watersheds located in the United States were selected
 for this study: Walnut Gulch (WG) in Arizona, Little Washita
 (LW) in Oklahoma, Little River (LR) in Georgia, and Reynolds
 Creek (RC) in Idaho (see Fig. 1). They represent different
 types of climate (from semiarid to humid) and land use patterns
 [47]. These four watersheds have been used as calibration and
 validation sites for comparison of AMSR-E satellite product
 [47] and SMOS product [38], [39].

WG is located in the Southeast Arizona. Most of the water-
 shed is covered by shrubs and grass, which is typical of the re-
 gion. The annual mean temperature is 17.6 °C (at Tombstone),
 and the annual mean precipitation is 320 mm (mainly from
 high intensity convective thunderstorms in the late summer).
 The uppermost 10 cm of the soil profile contains up to 60%
 gravel, and the underlying horizons usually contain less than
 40% gravel.

TABLE I
WATERSHED CHARACTERISTICS AND THE COORDINATES OF THE BOX CONTAINING THE POINTS USED FOR STATISTICS

Watershed	Number of stations	Climate	Annual rainfall (mm)	Topography	Land use	Box for statistics (corners coord.)
Walnut Gulch AZ	14	semi-arid	320	rolling	range	31.3 N - 110.5 W 32.3 N - 109.5 W
Little Washita OK	8	sub-humid	750	rolling	range/wheat	34.4 N - 98.5 W 35.4 N - 97.5 W
Little River GA	8	humid	1200	flat	row crop/forest	31.0 N - 84.0 W 32.0 N - 83.0 W
Reynolds Creek ID	15	semi-arid	500	mountainous	range	34.7 N - 98.7 W 35.7 N - 97.7 W

TABLE II
CORRELATION COEFFICIENTS (R) BETWEEN THE IN SITU MEASUREMENTS AT 130 AM AND 600 AM FOR THE FOUR WATERSHEDS. N IS THE NUMBER OF AVAILABLE DATES, AND CI IS THE 95% CONFIDENCE INTERVAL

WG			LW		
R	N	CI	R	N	CI
0.96	365	[0.95-0.97]	0.97	365	[0.96-0.98]
LR			RC		
R	N	CI	R	N	CI
0.95	365	[0.94-0.96]	0.99	328	[0.99-0.99]

288 LW is located in Southwest Oklahoma in the Southern Great
289 Plains region of the U.S. The climate is subhumid with an
290 average annual rainfall of 750 mm (mainly during the spring
291 and fall seasons). Topography is moderately rolling with a
292 maximum relief of less than 200 m. Land use is dominated by
293 rangeland and pasture (63%).

294 LR is located in the Southern Georgia near Tifton. With
295 an average annual precipitation of 1200 mm, the climate is
296 humid. The LR watershed is typical of the heavily vegetated
297 slow-moving stream systems in the Coastal Plain region of
298 the U.S. The topography over this watershed is relatively flat.
299 Approximately 40% of the watershed is forest with 40% crops
300 and 15% pasture.

301 RC is located in a mountainous area of Southwest Idaho. The
302 topography is high with a relief of over 1000 m that results in
303 diverse climates. Soils and vegetations are typical in this part
304 of the Rocky Mountains. The climate is considered as semiarid
305 with an annual precipitation of 500 mm. Approximately 75% of
306 the annual precipitation at high elevation is snow, whereas only
307 25% is snow at low elevation.

308 Surface soil moisture and temperature sensors (0–5 cm) have
309 been acquiring data since 2002 for the four watersheds. The
310 data used in this study are the means and standard deviations
311 of the soil moisture and surface temperature acquired every
312 30 min from 2009 to 2010 (hourly for RC). The averages
313 are based on 14/8/8/15 sensors for WG/LW/LR/RC, respec-
314 tively, after eliminating sensors with poor and suspicious
315 performances. Weighting coefficients have been derived for
316 each sensor with a Thiessen polygon. Table I summarizes the
317 characteristics of each watershed [47].

318 In order to estimate the effect of the rainfalls that could
319 occur between 130 am and 600 am, the correlation coefficients
320 between the measurements at 130 am and 600 am have been
321 computed for the four watersheds (see Table II and Fig. 2). They
322 range from 0.95 to 0.99, and based on the fact that rainfalls
323 would lower the correlation, we can assess that precipitations
324 that do not affect significantly the analysis.

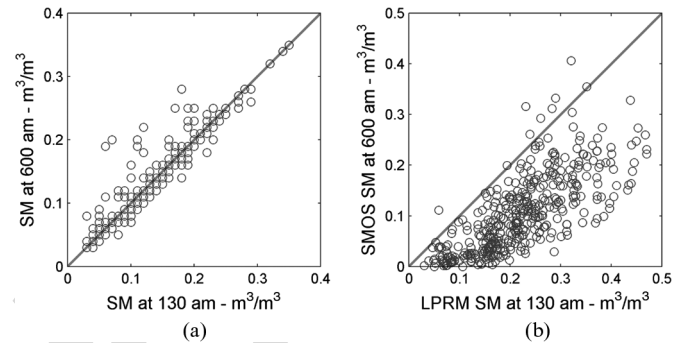


Fig. 2. Comparison between the 130 am and the 600 am soil moisture: *In situ* observations and satellite products for the four watersheds. (a) *In situ* soil moisture at 130 am and 600 am. (b) LPRM (130 am) and SMOS (600 am) soil moisture.

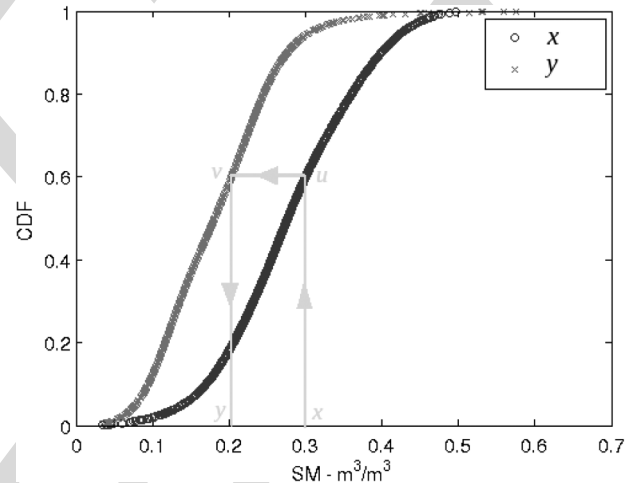


Fig. 3. Principle of CDF matching by setting the probabilities equal. For a given x , find y such that $G_Y(y) = F_X(x)$.

III. TWO STATISTICAL METHODS FOR GENERATING HOMOGENEOUS TIME SERIES

Two statistical methods were used to create a homogeneous time series of soil moisture. CDF matching has been widely used in previous studies to merge time series [14], [15], [18], [19], whereas copulas have just started to be used recently for environmental purposes.

A. CDF Matching

The CDF is the probability that a random variable X takes a value less than or equal to a given number x

$$F_X(x) = \Pr[X \leq x] \quad (1)$$

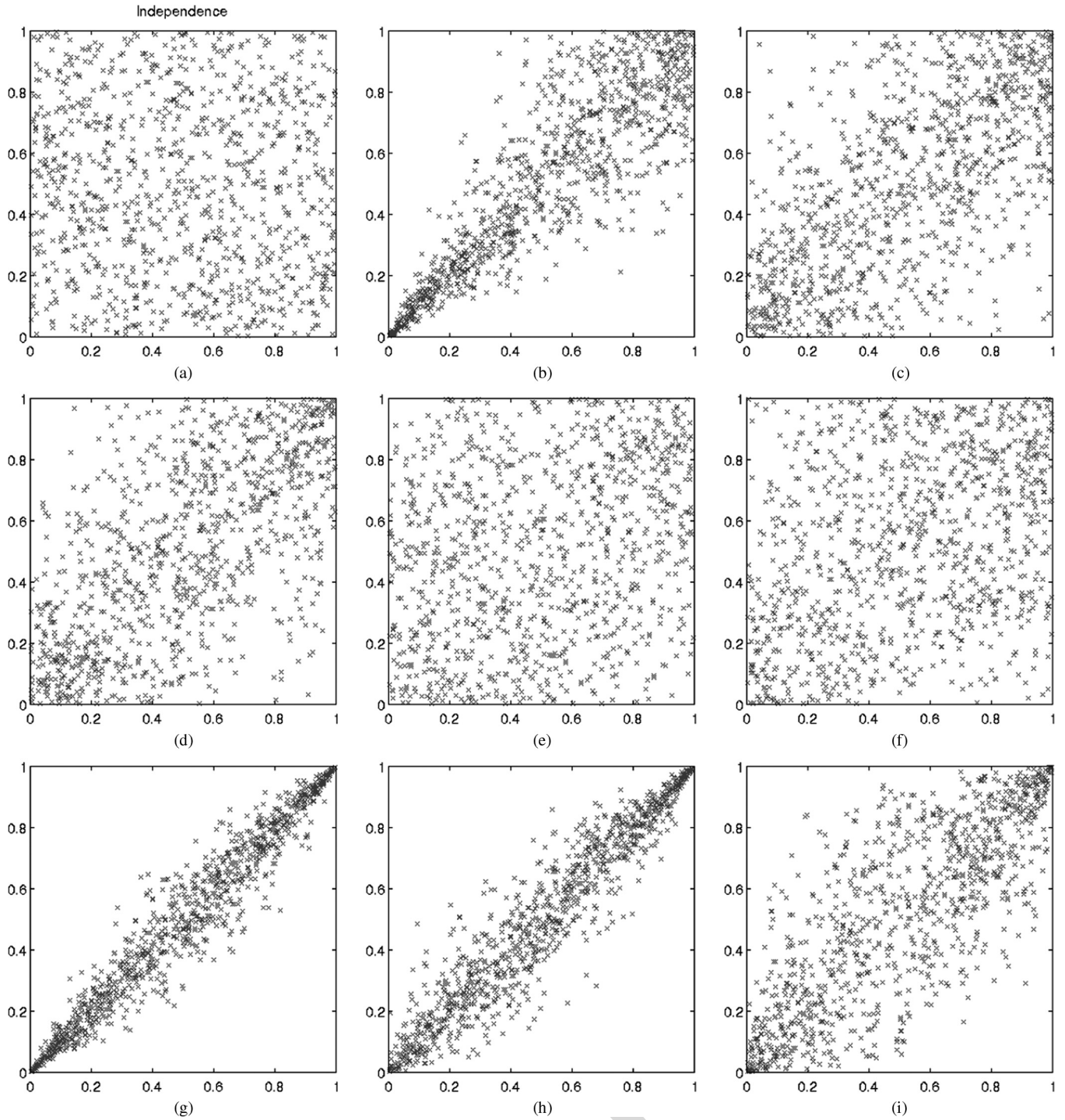


Fig. 4. Representations of the nine copulas showing their characteristics in the form of the point cloud (x -axis: CDF of the first data set; y -axis: CDF of the second data set).

335 where F_X is the CDF of the random variable X . If two time
 336 series are considered, the CDF matching consists of matching
 337 the CDF of each data set by setting their probabilities equal
 338 (see Fig. 3). The following approach has been applied here to
 339 the soil moisture data.

- 340 1) Compute the CDF of both data sets X and Y : F_X and G_Y .
- 341 2) Given a value x of X , find y such that $G_Y(y) = F_X(x)$.

342 However, the assumption that the probabilities $F_X(x)$ and
 343 $G_Y(y)$ are equal is never confirmed, and most of the time, they

are scattered like in Fig. 4. The copula method models this 344
 dependence between the probabilities. 345

For the rest of this paper, we use the variable u to represent 346
 $F_X(x)$ and v for $G_Y(y)$. U and V are data sets, whereas u and 347
 v are values of these data sets. 348

B. Copulas 349

The copula theory is a very useful and powerful tool to model 350
 the dependence structure between two sets of random variables. 351

TABLE III
NINE COPULAS TESTED IN THE STUDY: DEFINITION, PARAMETER RANGE, AND FAMILY

Copula	$C_\theta(u, v)$	$\theta \in$	Family
Independent	$u \cdot v$	-	-
Clayton	$(u^{-\theta} + v^{-\theta} - 1)^{-1/\theta}$	$(0, \infty)$	Archimedean
Frank	$-\frac{1}{\theta} \ln \left(1 + \frac{(e^{-\theta u} - 1)(e^{-\theta v} - 1)}{e^{-\theta} - 1} \right)$	$(-\infty, \infty)/0$	Archimedean
Gumbel	$\exp \left(- \left((-\ln u)^\theta + (-\ln v)^\theta \right)^{1/\theta} \right)$	$[1, \infty)$	Archimedean
FGM	$uv + \theta uv(1-u)(1-v)$	$[-1, 1]$	Elliptical
AMH	$\frac{uv}{1 - \theta(1-u)(1-v)}$	$[-1, 1]$	Archimedean
Arch12	$\left(1 + \left((u^{-1} - 1)^\theta + (v^{-1} - 1)^\theta \right)^{1/\theta} \right)^{-1}$	$[1, \infty)$	Archimedean
Arch14	$\left(1 + \left((u^{-1/\theta} - 1)^\theta + (v^{-1/\theta} - 1)^\theta \right)^{1/\theta} \right)^{-1/\theta}$	$[1, \infty)$	Archimedean
Gaussian	$\frac{\int_{-\infty}^{\phi^{-1}(u)} \int_{-\infty}^{\phi^{-1}(v)} \exp \left(\frac{2\theta s\omega - s^2 - \omega^2}{2(1-\theta^2)} \right)}{2\pi\sqrt{1-\theta^2}}$	$[-1, 1]$	Elliptical

352 Like the CDF matching, copulas separate the marginal behavior
353 of variables from the dependence structure by using distribution
354 functions. Instead of setting the probabilities u and v equal,
355 the variables U and V are compared and analyzed. The copula
356 function binds the two variables together.

357 There are many families of copulas which exhibit very differ-
358 ent properties. The form of the scatter of U and V is controlled
359 by the family choice, and the width of the tail of this scatter
360 is controlled by the single parameter θ . Most of the definitions
361 that follow in this section are based on [21].

362 1) *General Theory*: A copula is a function that gener-
363 ates a multivariate cumulative distribution function from 1-D
364 marginal CDFs. Given two random variables, X and Y , with
365 marginal CDFs F_X and G_Y , then, Sklar's theorem states

$$H_{XY}(x, y) = C_{XY}(F_X(x), G_Y(y)) = \Pr[X \leq x, Y \leq y] \quad (2)$$

366 where H_{XY} is the joint CDF of X and Y and C_{XY} is the asso-
367 ciated copula function. It is then possible to derive conditional
368 distributions, $H_{XY}(y|x)$, i.e., the joint CDF knowing x . Let
369 $u = F_X(x)$ and $v = G_Y(y)$. Then, $H_{XY}(y|x)$ can be derived by

$$C_{V|U} = \frac{\partial C(u, v)}{\partial u}. \quad (3)$$

370 Schweizer and Wolff [48] established that the copula func-
371 tion accounts for all the dependence between the two variables.
372 They demonstrated that transformations of the variables X and
373 Y do not affect their associated variables. Thus, the way that X
374 and Y evolve together is captured by the copula, regardless of
375 the scale in which each variable is measured.

376 2) *Some Copula Families*: The product copula corresponds
377 to the independence between X and Y

$$C(u, v) = u \cdot v. \quad (4)$$

378 A copula of the Archimedean family takes the following
379 form:

$$C(u, v) = \phi^{-1}(\phi(u) + \phi(v)) \quad (5)$$

380 where ϕ is the generator function that goes from $[0, 1]$ to
381 $(0, \infty)$. It satisfies three conditions: $\phi(1) = 0$, ϕ strictly de-
382 creasing, and ϕ convex.

383 Elliptical copulas have distributions with elliptic contours.
384 The main advantage of elliptical distributions is that the level

of correlation between the variables U and V can be specified. 385
The disadvantages are that elliptical copulas do not have closed- 386
form expressions and are restricted to have radial symmetry. 387

In this paper, nine copulas were used: the product cop- 388
ula, Clayton, Frank, Gumbel, Farlie–Gumbel–Moregenstern 389
(FGM), Ali–Mikhail–Haq, Arch12 (the 12th copula presented 390
in [21]), Arch14 (the 14th copula presented in [21]), and the 391
Gaussian copula. The nine copulas are described in Table III 392
and Fig. 4 and have their own characteristics. 393

- 1) Clayton: Strong left tail dependence and relatively weak 394
right tail dependence (i.e., u and v are strongly linked for 395
low values, whereas they are not for high values). 396
- 2) Frank: Dependence is symmetric in both tails, weak in 397
both tails, and stronger in the center of the distribution. 398
- 3) Gumbel: Strong right tail dependence and relatively weak 399
left tail dependence (the opposite of Clayton). 400
- 4) FGM: Useful when the dependence between U and V is 401
modest in amplitude. 402
- 5) Gaussian: Flexible as it allows for positive and negative 403
dependences. 404

Hafner and Reznikova [23] and Wang and Pham [49] 405
developed a method that includes the time into the copula 406
formula to create a dynamic copula evolving with time. In 407
this paper, time was not included, but the year 2010 was 408
divided into four seasons as different statistical behaviors were 409
expected: December–January–February, March–April–May 410
(MAM), June–July–August (JJA), and September–October– 411
November (SON). 412

3) *How to Select a Family*: Since copulas separate marginal 413
distributions from dependence structures, the appropriate cop- 414
ula for a particular application is the one that best captures the 415
dependence features of the data [22]. Dupuis [27] examined the 416
effects of model misspecification and highlighted the dangers 417
of improper copula selection. Genest and Rivest [50] proposed 418
a method to select the most appropriate copula, but this method 419
is only relevant for Archimedean copulas. Other methods 420
were developed to compare any type of copulas [51]–[54]. 421
Genest *et al.* [55] and Berg [54] compared some of them 422
and concluded that there was no universal test and that some 423
procedures performed better in some situations but never in all 424
the situations. 425

426 The method proposed by Huard *et al.* [56] is based on a
 427 Bayesian approach where any type of copula can be tested. It
 428 does not perform perfectly well in all the situations (with small
 429 correlation coefficients or with small sample size) but has the
 430 advantage to be a very fast method. This method was chosen
 431 in this study to select the copula that provides the best fit to the
 432 data.

433 4) *Method Used for Simulations:* The key to generating
 434 simulations from a copula is to understand that a copula is a
 435 joint distribution and that it obeys to the same rules. A con-
 436 ditional copula $C_{V|U}(u, v)$ is the probability that the random
 437 variable V is less than or equal to a value v knowing that the
 438 random variable U is equal to a value u

$$C_{V|U}(u, v) = \Pr[V \leq v | U = u] = t \sim \mathcal{U}(0, 1). \quad (6)$$

439 Simulating a uniform variable t is necessary in order to
 440 generate simulations from a copula. To retrieve $V|U$, the func-
 441 tion $C_{V|U}$ needs to be inverted such that $v = C_{V|U}^{-1}(t)$, or the
 442 equation $C_{V|U}(v) = t$ needs to be solved numerically. For each
 443 value of t , a value for v is retrieved. The following approach
 444 was used here to simulate data with the copulas.

- 445 1) Compute F_X and G_Y from the two original data sets X
 446 and Y with (1).
- 447 2) Choose the appropriate copula C by applying Huard's
 448 method and fitting the parameter θ to the original data.
- 449 3) Derive the conditional copula $C_{V|U}$ with (3).
- 450 4) Generate 1000 simulations $t \sim \mathcal{U}(0, 1)$.
- 451 5) Compute v with $v = C_{V|U}^{-1}(t)$ and y with $y = G_Y^{-1}(v)$.
- 452 6) The mean and standard deviation from the 1000 simula-
 453 tions can be computed.

454 IV. METHODOLOGY

455 For the CDF matching and the copula methods, 2010 data
 456 were used for calibration. The CDFs of SMOS and LPRM were
 457 calculated for the 2010 data sets. The two algorithms were then
 458 applied to the data from previous years. It should be noted that
 459 the consequence of using 2010 as a calibration year is that only
 460 the soil moisture range from 2010 is taken into account. If an
 461 extreme event occurred in the previous years, it might not be
 462 well described with these methods as they are only based on
 463 statistics and not on physical models. By looking at the *in situ*
 464 soil moisture time series in Fig. 7, 2010 did not have enough
 465 wet values over LR to estimate correctly the strong rainfalls
 466 of 2004, 2005, and 2009, not enough wet values over LW for
 467 rainfalls in 2007 and not enough dry values as well for 2003
 468 and 2006, and again not enough dry values over RC for all the
 469 previous years.

470 The two methods were applied to data contained in a $1^\circ \times 1^\circ$
 471 box around each watershed in order to have enough points for
 472 computing reliable statistics. The coordinates of each box are
 473 indicated in Table I. Only the satellite morning overpasses were
 474 selected for this study (6:00 am for SMOS and 1:30 am for
 475 AMSR-E, LST) since LPRM retrievals were only available for
 476 this overpass.

477 The 2010 calibration year was divided into four seasons:
 478 December–January–February, MAM, JJA, and SON. This

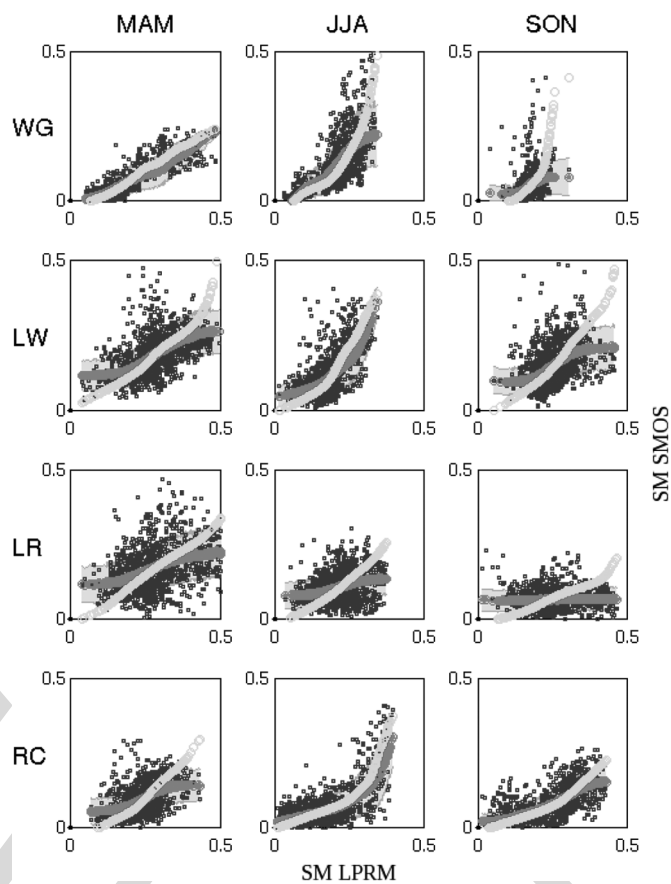


Fig. 5. Discrepancies in the simulations of soil moisture between CDF matching and copulas in 2010. Original soil moisture LPRM data are represented by blue points, and simulated data with CDF matching and copulas are in green and red, respectively. The standard deviation of the copula simulations is represented in shadowed red. Each row corresponds to a site, and each column corresponds to a season. *x*-axis: LPRM soil moisture. *y*-axis: SMOS soil moisture.

subdivision was done in order to better capture the sea-
 479 sonal dynamic that can be very different depending on the
 480 time of the year, particularly in vegetated areas. However,
 481 not enough points were available during the winter period
 482 (December–January–February) to compute reliable statistics,
 483 so no estimation was performed for this season. 484

When comparing either two different remote sensing prod-
 485 ucts or *in situ* data with remote sensing products, there is the
 486 issue of the scale effect, as the products may have significantly
 487 different spatial resolutions. Moreover, the spatial variability
 488 varies with the seasons and the heterogeneity. So as to reduce
 489 the problem, we used in this study averaged *in situ* data sets
 490 (8 to 15 stations that were several miles away) which were
 491 especially produced to be representative of 50-km spatial res-
 492 olution or so [47]. Also, statistics were applied to all the points
 493 contained in a $1^\circ \times 1^\circ$ box (more than 50 grid points). 494

495 V. GENERATED HOMOGENEOUS TIME SERIES

The year 2010 was used to compute the CDFs of each
 496 data set (SMOS and LPRM) for both methods and the joint
 497 CDF based on fitting and selecting copula functions as de-
 498 scribed previously. The soil moisture data were estimated using 499

TABLE IV
 STATISTICAL RESULTS OF THE SIMULATIONS FROM COPULAS AND CDF MATCHING. THE SIMULATIONS WERE COMPARED TO GROUND MEASUREMENTS OVER 2010 DIVIDED INTO FOUR SEASONS: MAM, JJA, SON, BUT NOT ENOUGH DATA AVAILABLE FOR WINTER SEASON. THE BEST RESULTS ARE WRITTEN IN BOLD, AND RMSES ARE IN m^3/m^3

		SMOS		LPRM		Copula method			CDF matching		# points
		R	RMSE	R	RMSE	Fam(θ)	R	RMSE	R	RMSE	
WG	MAM	0.80	0.032	0.82	0.125	Gumbel (2.18)	0.89	0.020	0.87	0.031	43
	JJA	0.86	0.053	0.86	0.126	Clayton(2.63)	0.76	0.076	0.81	0.090	45
	SON	0.64	0.029	0.79	0.133	Frank (3.13)	0.64	0.012	0.53	0.029	42
	total	0.84	0.040	0.79	0.139	-	0.79	0.043	0.82	0.054	159
LW	MAM	0.70	0.068	0.48	0.166	Frank (4.40)	0.55	0.057	0.57	0.075	44
	JJA	0.85	0.037	0.58	0.085	Gumbel (1.66)	0.77	0.042	0.76	0.050	44
	SON	0.80	0.041	0.80	0.122	Frank (3.61)	0.75	0.023	0.72	0.048	46
	total	0.78	0.049	0.59	0.148	-	0.71	0.043	0.71	0.059	162
LR	MAM	0.77	0.080	0.54	0.175	Frank (2.82)	0.59	0.063	0.58	0.067	39
	JJA	0.57	0.053	0.67	0.131	Frank (2.00)	0.65	0.034	0.66	0.033	40
	SON	0.59	0.032	0.37	0.174	FGM (0.31)	0.17	0.033	0.16	0.037	39
	total	0.74	0.060	0.65	0.178	-	0.51	0.045	0.59	0.048	147
RC	MAM	0.14	0.097	0.11	0.096	Frank (3.10)	0.26	0.089	0.27	0.105	47
	JJA	0.63	0.055	0.81	0.070	Gumbel (1.81)	0.84	0.047	0.83	0.052	42
	SON	0.14	0.070	0.52	0.144	Frank (6.30)	0.34	0.056	0.29	0.066	39
	total	0.55	0.081	0.73	0.099	-	0.80	0.059	0.70	0.067	142

500 the conditional distribution (conditional on LPRM retrievals).
 501 While the copula procedure has the potential to generate an
 502 ensemble of SMOS-like soil moisture estimates, given the
 503 LPRM estimated soil moisture, we only use the mean estimate.
 504 The ensembles could be used to provide uncertainty estimates.
 505 It should be noted that CDF matching can only provide a
 506 single SMOS estimate. The resulting time series will result in
 507 a statistically homogeneous time series under the assumption
 508 that 2010 LPRM retrievals and the underlying AMSR-E bright-
 509 ness temperatures are temporally consistent. The resulting
 510 SMOS-like estimated soil moisture is then compared to ground
 511 measurements.

512 A. Calibration Year 2010 and Comparison With 513 Ground Measurements

514 2010 is the year with both SMOS data and LPRM data.
 515 CDFs were computed for both variables. CDF matching and
 516 copula methods were then applied, and these produced different
 517 SMOS-like estimates. In Fig. 5, the original data (SMOS and
 518 LPRM) are represented by the blue point cloud, CDF matching
 519 and copula estimates are in green and red colors, respectively,
 520 and standard deviations from copula simulations are in red
 521 shadows. This standard deviation can be interpreted as the
 522 uncertainty associated to the copula simulations, which can be
 523 not produced by CDF matching estimation.

524 Over WG in the MAM season, there was no obvious differ-
 525 ence between the two simulation methods. However, in the JJA
 526 and SON seasons, there were differences for the high values
 527 of soil moisture: The CDF matching method produced higher
 528 simulated values than the copula method. Similar behavior can
 529 also be seen for all seasons in the other three sites, i.e., LW, LR,
 530 and RC. Discrepancies can also be observed for small values
 531 of soil moisture over LW, LR, and RC (MAM) where copulas
 532 generated higher values of soil moisture.

533 Standard deviations of soil moisture simulations from copu-
 534 las were also computed (see Fig. 5). This standard deviation is
 535 directly related to the width of the tail of the chosen copula
 536 which is controlled by the θ parameter. A high value of the
 537 standard deviation corresponds to a large tail, meaning that

the two variables are weakly linked to each other, whereas a 538
 small value corresponds to a strong link. The differences in 539
 the simulations can also be observed in the 2010 time series 540
 (see Table IV and Fig. 6). Compared to the original LPRM 541
 data, the estimated soil moisture was close to the SMOS level 542
 and comparable to the ground measurements. The bias between 543
 LPRM and SMOS was corrected by both methods. 544

Over WG, CDF matching and copula simulations were not 545
 very different except in the summer season when the CDF 546
 matching simulations were higher than the copulas. Consid- 547
 ering the entire year, both simulation methods improved the 548
 original statistics from the LPRM data set. The correlation 549
 coefficient did not change significantly ($R = 0.79$ for LPRM 550
 and $R = 0.79/0.82$ for copulas/CDF matching), but the rmse 551
 was highly improved going from $0.139 \text{ m}^3/\text{m}^3$ (original LPRM 552
 data) to $0.054 \text{ m}^3/\text{m}^3$ with CDF matching and $0.043 \text{ m}^3/\text{m}^3$ 553
 with copula, which represents an improvement of a factor of 3. 554

Over LW, simulations responded very well to the succes- 555
 sive rain events throughout the year and exhibited a pattern 556
 of decrease following a rain event. The first two months 557
 (March–April) exhibited more noisy simulations, and the statis- 558
 tics were impacted by this behavior ($R = 0.55/0.57$ and 559
 $\text{rmse} = 0.057/0.075 \text{ m}^3/\text{m}^3$ for copulas/CDF matching). The 560
 other two seasons gave good results in terms of statistics. For 561
 the entire year, the R value was highly improved ($R = 0.59$ 562
 for LPRM and $R = 0.71/0.71$ for copulas/CDF matching), and 563
 the rmse was reduced by a factor of 3 ($\text{rmse} = 0.148 \text{ m}^3/\text{m}^3$ 564
 for LPRM and $\text{rmse} = 0.043/0.059 \text{ m}^3/\text{m}^3$ for copulas/CDF 565
 matching). 566

The LR watershed is the site with the highest rainfall fre- 567
 quency (events of small amplitude). The successive rainfall 568
 events were not well captured by the simulations, particularly 569
 during the fall season when both simulations exhibited only 570
 small variations, which resulted in very poor statistics ($R =$ 571
 $0.17/0.16$ for copulas/CDF matching). Unfortunately, even if 572
 the rain events were captured by the original data sets, none 573
 was captured by both data sets at the same time, so only the 574
 nonraining periods were taken into account by the statistics. 575
 Therefore, the simulations can only be representative of the dry 576
 periods. It should be noted that the statistics of LPRM were 577

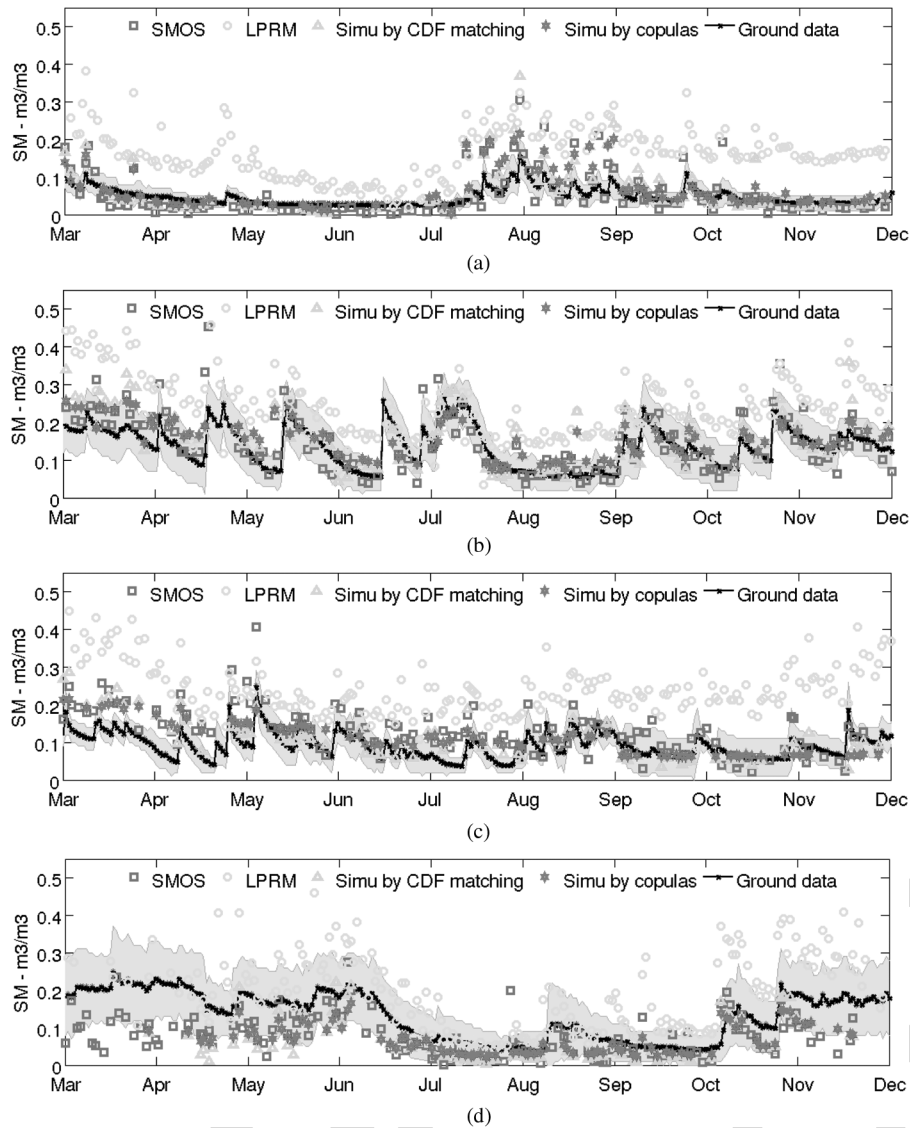


Fig. 6. Simulations for 2010: SMOS, LPRM, simulated soil moisture data from CDF matching and copulas, and ground measurements over the four watersheds. Since the *in situ* data are the mean of several ground measurements, their standard deviations are represented in gray shadows showing the spatial variability. (a) WG. (b) LW. (c) LR. (d) RC.

578 already not good during this season ($R = 0.37$ and $rmse =$
 579 $0.174 \text{ m}^3/\text{m}^3$). During the spring season, SMOS overestimated
 580 the *in situ* soil moisture measurements, so as a result, the
 581 copulas and CDF matching estimates overestimated the *in situ*
 582 measurements as well.

583 RC is located in a mountainous region and is subject to
 584 frequent snow and frozen soil events. The satellite-based soil
 585 moisture was not comparable to the ground measurements until
 586 late May. After this winter period, the simulations captured
 587 accurately the soil moisture evolution and improved the original
 588 statistics and especially the $rmse$ ($0.099 \text{ m}^3/\text{m}^3$ for LPRM and
 589 $0.059/0.067 \text{ m}^3/\text{m}^3$ for copulas/CDF matching).

590 *B. Times Series 2003–2010 and Comparison With*
 591 *Ground Measurements*

592 Soil moisture from 2003 to 2010 was simulated from the
 593 LPRM retrievals (2003–2010) using the copulas and CDF

matching relationships developed for 2010. Fig. 7 and Table V
 594 show the entire time series and the associated statistics (R and
 595 $rmse$) between the original data, CDF matching simulations,
 596 copula simulations, and ground measurements. 597

WG is the driest site and did not have a lot of rain events.
 598 These rain events were well described by the simulated soil
 599 moisture even though they were sometimes largely overesti-
 600 mated, particularly by CDF matching simulations. Artifacts at
 601 the extremities of the seasons can be seen at the beginning
 602 of 2006 and 2008. The correlation coefficient was improved
 603 using the CDF matching for each year, whereas the errors were
 604 reduced by a factor larger than 2 with the copulas. 605

The overestimation of the soil moisture after the rain events
 606 with CDF matching can be found as well over LW, but the
 607 temporal evolution was well captured by both methods. For this
 608 watershed, CDF matching overestimated the high soil moisture
 609 values and underestimated the low values. CDF matching pro-
 610 duced soil moisture with a higher dynamic range than copulas.
 611

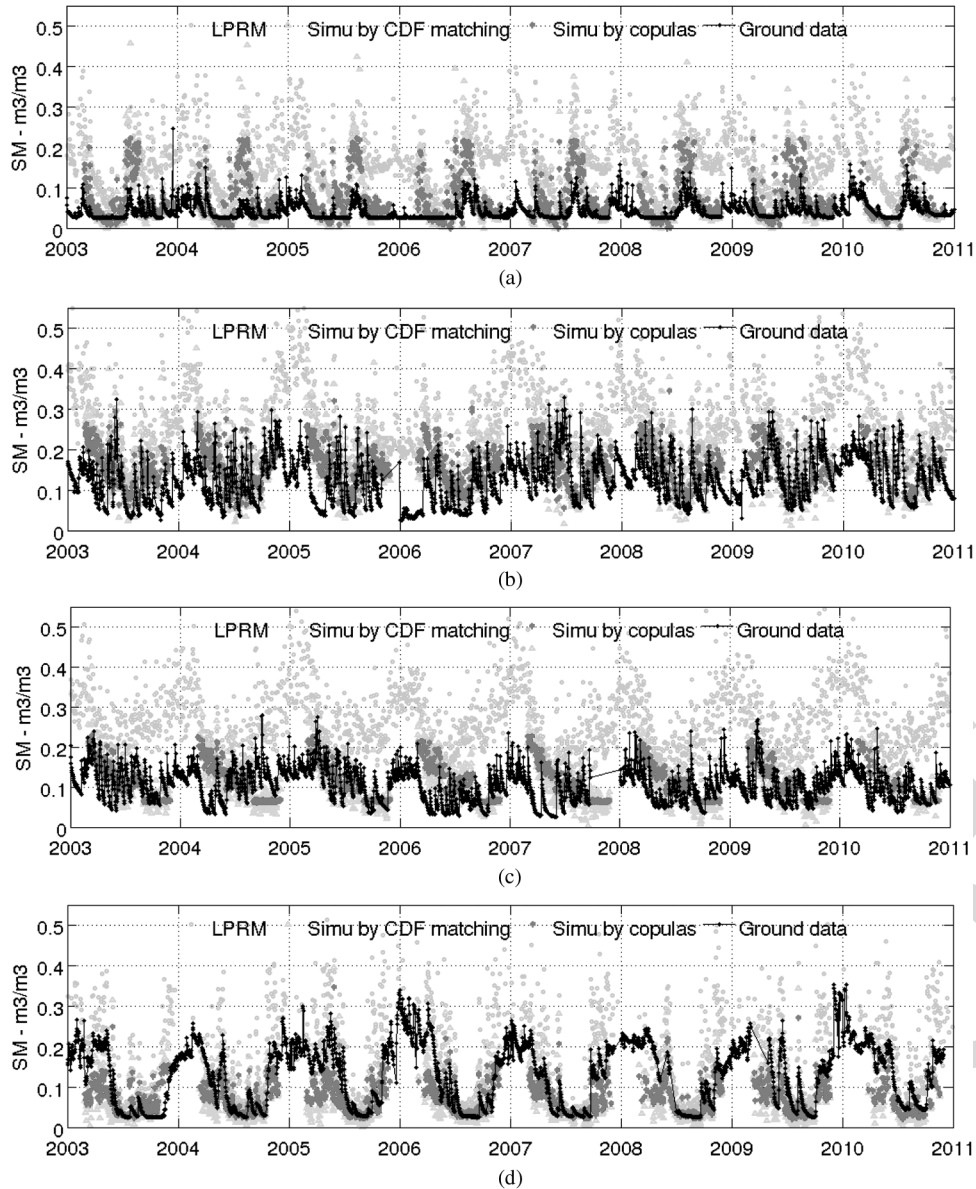


Fig. 7. Simulated time series from 2003 to 2010 with ground measurements for the four watersheds. (a) WG. (b) LW. (c) LR. (d) RC.

612 This was reflected in the total rmse value ($0.079 \text{ m}^3/\text{m}^3$),
 613 whereas the rmse of the copula simulations was of $0.066 \text{ m}^3/\text{m}^3$
 614 (original LPRM rmse: $0.160 \text{ m}^3/\text{m}^3$).

615 LR is the site with the largest number of rain events, and as
 616 mentioned in the previous section, this high rain frequency was
 617 not properly captured during the fall season of 2010; this can
 618 be seen as well in the entire time series where all the copulas
 619 and CDF matching estimates were flat during fall seasons.
 620 Moreover, since SMOS was overestimating the soil moisture
 621 during the spring season of 2010, both statistical estimates had
 622 this behavior. Even though the tendency of the simulations was
 623 correct, the dynamic behavior was not well represented, which
 624 resulted in a very poor correlation coefficient (negative values
 625 in 2004 and 2007).

626 RC is a very complicated site because of the frequent
 627 snow and frozen soil events occurring during half of the year.
 628 However, statistical results were improved for the entire year

with copula simulations (rmse = $0.099 \text{ m}^3/\text{m}^3$ for LPRM and
 629 rmse = $0.056/0.062 \text{ m}^3/\text{m}^3$ for copulas/CDF matching). 630

VI. CONCLUSION AND PERSPECTIVES 631

The main goal of this study was to propose a new method to
 632 generate a long homogeneous time series (2003–2010) of soil
 633 moisture from two overlapping time series. 634

For that purpose, two statistical tools, the CDF matching and
 635 the copulas, were tested over four watersheds in the U.S. By us-
 636 ing CDF matching, the assumption that the two studied data sets
 637 are ranked in the same way is made, which the copulas do not
 638 require. The two analyzed data sets (SMOS and LPRM) were
 639 jointly available only for 2010, so data from 2010 were used to
 640 estimate the CDFs that are used as references to estimate SMOS
 641 soil moisture for previous years. The novelty of the approach is
 642 its application: establishing the statistical relationship between 643

TABLE V
 STATISTICAL RESULTS FROM THE COMPARISON BETWEEN THE SIMULATED TIME SERIES OF SOIL MOISTURE FROM 2003 TO 2010. ORIGINAL SOIL MOISTURE TIMES ARE REPRESENTED BY LPRM. THE BEST RESULTS ARE INDICATED IN BOLD, AND THE RMSE ARE IN m^3/m^3 . (a) WG. (b) LW. (c) LR. (d) RC

		(a)								
		2003	2004	2005	2006	2007	2008	2009	2010	Total
LPRM	R	0.070	0.76	0.82	0.66	0.81	0.68	0.65	0.79	0.73
	RMSE	0.129	0.141	0.146	0.133	0.147	0.138	0.129	0.139	0.138
Copula	R	0.62	0.55	0.82	0.64	0.81	0.75	0.76	0.79	0.69
	RMSE	0.059	0.059	0.059	0.060	0.054	0.053	0.060	0.043	0.057
CDF m.	R	0.73	0.62	0.88	0.72	0.89	0.75	0.79	0.82	0.74
	RMSE	0.070	0.074	0.071	0.073	0.067	0.067	0.077	0.054	0.071

		(b)								
		2003	2004	2005	2006	2007	2008	2009	2010	Total
LPRM	R	0.56	0.71	0.48	0.67	0.32	0.42	0.52	0.58	0.55
	RMSE	0.163	0.149	0.187	0.149	0.173	0.158	0.149	0.149	0.160
Copula	R	0.56	0.47	0.19	0.62	0.41	0.64	0.58	0.71	0.47
	RMSE	0.071	0.064	0.088	0.077	0.060	0.056	0.051	0.044	0.066
CDF m.	R	0.59	0.60	0.34	0.63	0.49	0.61	0.53	0.71	0.51
	RMSE	0.083	0.070	0.101	0.092	0.069	0.076	0.069	0.059	0.079

		(c)								
		2003	2004	2005	2006	2007	2008	2009	2010	Total
LPRM	R	0.51	0.60	0.46	0.75	0.64	0.70	0.49	0.65	0.58
	RMSE	0.171	0.148	0.181	0.185	0.180	0.166	0.187	0.178	0.174
Copula	R	0.54	-0.48	0.73	0.01	-0.14	0.20	0.43	0.51	0.19
	RMSE	0.042	0.079	0.036	0.069	0.081	0.054	0.047	0.045	0.059
CDF m.	R	0.68	-0.16	0.72	0.28	0.18	0.50	0.55	0.59	0.37
	RMSE	0.044	0.080	0.042	0.070	0.085	0.050	0.048	0.048	0.061

		(d)								
		2003	2004	2005	2006	2007	2008	2009	2010	Total
LPRM	R	0.78	0.76	0.74	0.80	0.84	0.69	0.78	0.73	0.77
	RMSE	0.093	0.085	0.110	0.099	0.102	0.106	0.099	0.099	0.099
Copula	R	0.53	0.78	0.70	0.68	0.72	0.75	0.72	0.80	0.69
	RMSE	0.065	0.045	0.065	0.060	0.051	0.047	0.052	0.059	0.056
CDF m.	R	0.42	0.69	0.65	0.63	0.70	0.65	0.71	0.70	0.63
	RMSE	0.073	0.051	0.070	0.063	0.055	0.056	0.056	0.067	0.062

644 AMSR-E and SMOS retrieved soil moisture values and using
 645 this relationship to estimate the *equivalent* SMOS value for the
 646 AMSR-E period prior to the SMOS launch.

647 The first analysis of these simulations over 2010 showed that
 648 the simulated data sets were very similar to the SMOS estimates
 649 and reproduced SMOS behavior accurately except over the LR
 650 watershed where numerous rain events occurred. This high
 651 rainfall frequency was interpreted statistically as noise, and
 652 hence, the simulations did not describe the soil moisture evolu-
 653 tion over this site very well. RC was also a very complicated site
 654 due to the local topography and seasonal climate conditions.
 655 Soil moisture derived from satellite observations was not able
 656 to accurately reproduce the dynamics as found in the *in situ*
 657 data, and as a result, the simulated soil moisture did not either.
 658 However, the total rmse for the simulated soil moisture from
 659 copulas was reduced by a factor of almost 2. The WG and
 660 LW sites were well represented by the simulations, and copulas
 661 improved the error by a factor of 3, whereas CDF matching
 662 improved the correlation.

663 The time series of soil moisture were estimated from 2003 to
 664 2010 and were compared to *in situ* measurements at all four
 665 watersheds. Since simulated soil moisture data in 2010 over
 666 the LR watershed had very little dynamic range, they remained
 667 the same for the entire time series and showed very poor
 668 statistical results. Even though the rmse values were improved

by a factor of 3, the total correlation was not good. For the
 three other sites, the correlation coefficient was a bit degraded
 compared to the original LPRM data, but the rmse was highly
 improved with copulas by a factor of 2 to 3. In general, CDF
 matching gave better results in terms of correlation, and copulas
 gave better results in terms of errors compared to the ground
 measurements.

As a more general conclusion, CDF matching gives good
 results but does not take into account the structure of the
 dependence between the two data sets, whereas the copulas
 allow to model this structure. Through the choice of the family
 and the parameter θ (which controls the width of the tail of the
 scatter), it is possible to model all kinds of structures, from the
 perfect dependence (CDF matching), right or left dependence,
 to complete independence. This is why copulas produce better
 results for the extreme values (very low and very high values)
 than CDF matching. Copulas can also estimate the uncertainty
 of the soil moisture simulations given the LPRM value and
 can be seen as a quality information in the simulation process.
 However, the copula method is time consuming. It is quick
 to choose the copula family and its associated parameter as
 it is based on a Bayesian approach; however, it is very time
 consuming to generate the 1000 simulations, particularly if the
 chosen copula does not have an analytic inversion form. In the
 latter case, 1000 equations need to be resolved numerically.

694 Nevertheless, these simulations represent an advantage since it
695 is possible to compute a mean and a standard deviation. The
696 limitations are the same for both methods and even for any
697 general statistical methods using a specific year as a reference:
698 Only the variable range of this particular year can be well
699 represented. Therefore, if an event in a previous year occurs
700 and is out of the range found in the specific year of reference
701 (such as drought or flood events), then that event will not be
702 well represented in the simulated results.

703 In order to improve this methodology, applying a moving
704 window of three months would provide more accurate results
705 instead of dividing the year into four seasons. This would also
706 avoid the artifacts and gaps generally noticed at the transition
707 between the seasons. Another solution would be to introduce
708 the time in the copulas, but the level of complexity in the copula
709 manipulation would increase as well.

710 In this paper, the attempt to build a homogeneous soil mois-
711 ture time series has been based on statistical methods only. Of
712 course, other methods exist to reconcile different sensor ac-
713 quisitions, and because SMOS and AMSR-E do not operate at
714 the same frequencies and not at the same crossing times, using
715 physical models to tackle these discrepancies is an alternative to
716 statistical methods. Moreover, matching observations acquired
717 at 130 am and 600 am can trigger some questions, particularly
718 regarding the precipitations that could occur in between. The
719 present study is a first step toward a unified and homogeneous
720 soil moisture time series, and mixing physical and statisti-
721 cal models to do so would be a breakthrough for climate
722 studies.

723 The next step of this study is to build a homogeneous time
724 series of soil moisture at the global scale. Hence, the results of
725 this study will be extended in the future to build a global map
726 of the copula family choice and to study if there exists any rela-
727 tionship between the chosen copulas and the soil characteristics
728 or land use data. This would allow us to derive soil moisture
729 time series from LPRM data within SMOS soil moisture range
730 over the entire globe.

731 ACKNOWLEDGMENT

732 The authors would like to thank the USDA research team for
733 providing the *in situ* data and D. Huard from McGill University
734 for the helpful inputs on the copula method. USDA is an Equal
735 Employment Opportunity employer.

736 REFERENCES

737 [1] "Implementation Plan for the Global Observing System for Climate
738 in Support of the UNFCCC," World Meteorological Org., Geneva,
739 Switzerland, Tech. Rep., 2010.
740 [2] M. Drusch, "Initializing numerical weather predictions models with satel-
741 lite derived surface soil moisture: Data assimilation experiments with
742 ECMWF's integrated forecast system and the TMI soil moisture data set,"
743 *J. Geophys. Res.*, vol. 113, no. D3, p. D03 102, Feb. 2007.
744 [3] H. Douville and F. Chauvin, "Relevance of soil moisture for seasonal cli-
745 mate predictions: A preliminary study," *Climate Dyn.*, vol. 16, no. 10/11,
746 pp. 719–736, Oct. 2000.
747 [4] Y. Kerr, P. Waldteufel, J. Wigneron, S. Delwart, F. Cabot, J. Boutin,
748 M. Escorihuela, J. Font, N. Reul, C. Gruhier, S. Juglea, M. Drinkwater,
749 A. Hahne, M. Martin-Neira, and S. Mecklenburg, "The SMOS mission:
750 New tool for monitoring key elements of the global water cycle," *Proc.*
751 *IEEE*, vol. 98, no. 5, pp. 666–687, May 2010.

[5] D. Entekhabi, E. Njoku, P. O'Neill, K. Kellogg, W. Crow, W. Edelstein, 752
J. Entin, S. Goodman, T. Jackson, J. Johnson, J. Kimball, J. Piepmeier, 753
R. Koster, N. Martin, K. McDonald, M. Moghaddam, S. Moran, 754
R. Reichle, J. Shi, M. Spencer, S. Thurman, L. Tsang, and J. Zyl, "The 755
soil moisture active passive (SMAP) mission," *Proc. IEEE*, vol. 98, no. 5, 756
pp. 704–716, May 2010.
[6] Y. Kerr, P. Waldteufel, J. Wigneron, J. Martinuzzi, J. Font, and M. Berger, 757
"Soil moisture retrieval from space: The soil moisture and ocean salinity 759
(SMOS) mission," *IEEE Trans. Geosci. Remote Sens.*, vol. 39, no. 8, 760
pp. 1729–1735, Aug. 2001.
[7] M. Owe, R. de Jeu, and J. Walker, "A methodology for surface soil 762
moisture and vegetation optical depth retrieval using the microwave pol- 763
arization difference index," *IEEE Trans. Geosci. Remote Sens.*, vol. 39, 764
no. 8, pp. 1643–1654, Aug. 2001.
[8] E. Njoku, T. Jackson, V. Lakshmi, T. Chan, and S. Nghiem, "Soil moisture 766
retrieval from AMSR-E," *IEEE Trans. Geosci. Remote Sens.*, vol. 41, 767
no. 2, pp. 215–229, Feb. 2003.
[9] L. Li, P. Gaiser, B. Gao, R. Bevilacqua, T. Jackson, E. Njoku, C. Rüdiger, 769
J. Calvet, and R. Bindlish, "Windsat global soil moisture retrieval and 770
validation," *IEEE Trans. Geosci. Remote Sens.*, vol. 48, no. 5, pp. 2224– 771
2241, May 2010.
[10] V. Naeimi, K. Scipal, Z. Bartalis, and S. H. W. Wagner, "An improved soil 773
moisture retrieval algorithm for ERS and METOP scatterometer observa- 774
tions," *IEEE Trans. Geosci. Remote Sens.*, vol. 47, no. 7, pp. 1999–2013, 775
Jul. 2009.
[11] L. Vincent, X. Zhang, B. Bonsal, and W. Hogg, "Homogenization of 777
daily temperatures over Canada," *J. Climate*, vol. 15, no. 11, pp. 1322– 778
1334, Jun. 2002.
[12] M. Begert, T. Schlegel, and W. Kirchhofer, "Homogeneous temperature 780
and precipitation series of Switzerland from 1864 to 2000," *Int. J. Clima- 781
tol.*, vol. 25, no. 1, pp. 65–80, Jan. 2005.
[13] G. Picard and M. Fily, "Surface melting observations in Antarctica by 783
microwave radiometers: Correcting 26-year time series from changes in 784
acquisition hours," *Remote Sens. Environ.*, vol. 104, no. 3, pp. 325–336, 785
Oct. 2006.
[14] R. Reichle and R. Koster, "Bias reduction in short records of satellite soil 787
moisture," *Geophys. Res. Lett.*, vol. 31, no. 19, p. L19 501, Oct. 2004. 788
[15] M. Choi and J. Jacobs, "Temporal variability corrections for advanced 789
microwave scanning radiometer E (AMSR-E) surface soil moisture: 790
Case study in little river region, Georgia, U.S.," *Sensors*, vol. 8, no. 4, 791
pp. 2617–2627, Apr. 2008.
[16] H. Li, J. Sheffield, and E. Wood, "Bias correction of monthly precipitation 793
and temperature fields from IPCC AR4 models using equidistant quantile 794
matching," *J. Geophys. Res., Atmosp.*, vol. 115, no. D10, p. D10 101, 795
May 2010.
[17] M. Drusch, E. Wood, and H. Gao, "Observation operators for the di- 797
rect assimilation of TRMM microwave imager retrieved soil moisture," 798
Geophys. Res. Lett., vol. 32, no. 15, p. L15 403, Aug. 2005. 799
[18] Y. Liu, A. van Dijk, R. de Jeu, and T. Holmes, "An analysis of spatiotem- 800
poral variations of soil and vegetation moisture from a 29-year satellite- 801
derived data set over mainland Australia," *Water Resour. Res.*, vol. 45, 802
no. 7, p. W07 405, Jul. 2009. 803
[19] Y. Liu, R. Parinussa, W. Dorigo, R. D. Jeu, W. Wagner, A. V. Dijk, 804
M. McCabe, and J. Evans, "Developing an improved soil moisture dataset 805
by blending passive and active microwave satellite-based retrievals," 806
Hydrol. Earth Syst. Sci., vol. 15, no. 2, pp. 425–436, Feb. 2011. 807
[20] V. Singh and W. Strupczewski, "Editorial," *J. Hydrol. Eng.*, vol. 12, no. 4, 808
p. 345, Jul. 2007. 809
[21] R. Nelsen, "An introduction to copulas," in *Springer Series in Statistics*. 810
New York, NY, USA: Springer-Verlag, 1998. 811
[22] P. Trivedi and D. Zimmer, *Copula Modeling: An Introduction for Practi- 812
tioners*, vol. 1, *Foundations and Trends in Econometrics*. Hanover, MA, 813
USA: Now Publ. Inc., 2005, pp. 1–111. 814
[23] C. Hafner and O. Reznikova, "Efficient estimation of a semiparametric 815
dynamic copula model," *Comput. Stat. Data Anal.*, vol. 54, no. 11, 816
pp. 2609–2627, Nov. 2010. 817
[24] C. Genest and A. Favre, "Everything you always wanted to know about 818
copula modeling but were afraid to ask," *J. Hydrol. Eng.*, vol. 12, no. 4, 819
pp. 347–368, Jul./Aug. 2007. 820
[25] A. Favre, S. E. Adlouni, L. Perreault, N. Thiémond, and B. Bobée, "Mul- 821
tivariate hydrological frequency analysis using copulas," *Water Resour.* 822
Res., vol. 40, no. 1, p. W01 101, Jan. 2004. 823
[26] G. Salvadori and C. de Michele, "On the use of copulas in hydrology: 824
Theory and practice," *J. Hydrol. Eng.*, vol. 12, no. 4, pp. 369–380, 825
Jul. 2007. 826
[27] D. Dupuis, "Using Copulas in hydrology: Benefits, cautions and issues," 827
J. Hydrol. Eng., vol. 12, no. 4, pp. 381–393, Jul. 2007. 828

829 [28] L. Zhang and V. Singh, "Trivariate flood frequency analysis using the
830 Gumbel-Hougaard copula," *J. Hydrol. Eng.*, vol. 12, no. 4, pp. 431–439,
831 Jul. 2007.

832 [29] F. Serinaldi and S. Grimaldi, "Fully nested 3-copula: Procedure and appli-
833 cation on hydrological data," *J. Hydrol. Eng.*, vol. 12, no. 4, pp. 420–430,
834 Jul. 2007.

835 [30] P. Laux, S. Vogl, W. Qiu, H. Knoche, and H. Kunstmann, "Copula-based
836 statistical refinement of precipitation in RCM simulations over complex
837 terrain," *Hydrol. Earth Syst. Sci.*, vol. 15, no. 7, pp. 2401–2419, Jul. 2011.

838 [31] H. Gao, E. Wood, M. Drusch, and M. McCabe, "Copula-derived observa-
839 tion operators for assimilating TMI and AMSR-E retrieved soil moisture
840 into land surface models," *J. Hydrometeorol.*, vol. 8, no. 3, pp. 413–429,
841 Jun. 2007.

842 [32] C. de Michele and G. Salvadori, "A generalized pareto intensity-duration
843 model of storm rainfall exploiting 2-copulas," *J. Geophys. Res.*, vol. 108,
844 no. D2, p. 4067, Jan. 2003.

845 [33] J. Wigneron, Y. Kerr, P. Waldteufel, K. Saleh, M. Escorihuela,
846 P. Richaume, P. Ferrazzoli, P. de Rosnay, R. Gurney, J. Calvet, J. Grant,
847 M. Guglielmetti, B. Hornbuckle, C. Mätzler, T. Pellarin, and M. Schwank,
848 "L-band microwave emission of the biosphere (L-MEB) model: Descrip-
849 tion and calibration against experimental data sets over crop fields,"
850 *Remote Sens. Environ.*, vol. 107, no. 4, pp. 639–655, Apr. 2007.

851 [34] Y. Kerr, P. Waldteufel, P. Richaume, J. Wigneron, P. Ferrazzoli,
852 A. Mahmoodi, A. A. Bitar, F. Cabot, C. Gruhier, S. Juglea, D. Leroux,
853 A. Mialon, and S. Delwart, "The SMOS soil moisture retrieval algo-
854 rithm," *IEEE Trans. Geosci. Remote Sens.*, vol. 50, no. 5, pp. 1384–1403,
855 May 2012.

856 [35] D. Carr, R. Kahn, K. Sahr, and T. Olsen, "ISEA discrete global grids,"
857 *Stat. Comput. Stat. Graph. Newl.*, vol. 8, no. 2/3, pp. 31–39, 1997.

858 [36] A. A. Bitar, D. Leroux, Y. Kerr, O. Merlin, P. Richaume, A. Sahoo, and
859 E. Wood, "Evaluation of SMOS soil moisture products over continental
860 US using SCAN/SNOTEL network," *IEEE Trans. Geosci. Remote Sens.*,
861 vol. 50, no. 5, pp. 1572–1586, May 2012.

862 [37] G. Schaefer, M. Cosh, and T. Jackson, "The USDA natural resources
863 conservation service soil climate analysis network (SCAN)," *J. Atmosf.*
864 *Ocean. Technol.*, vol. 24, no. 12, pp. 2073–2077, Dec. 2007.

865 [38] T. Jackson, R. Bindlish, M. Cosh, T. Zhao, P. Starks, D. Bosch,
866 M. Seyfried, S. Moran, Y. Kerr, and D. Leroux, "Validation of soil mois-
867 ture and ocean salinity (SMOS) soil moisture over watershed networks in
868 the U.S.," *IEEE Trans. Geosci. Remote Sens.*, vol. 50, no. 5, pp. 1530–
869 1543, May 2012.

870 [39] D. Leroux, Y. Kerr, A. A. Bitar, C. Gruhier, R. Bindlish, T. Jackson,
871 B. Berthelot, and G. Portet, "Comparison between SMOS, VUA, ASCAT
872 and ECMWF soil moisture products over four watersheds in the U.S.,"
873 *IEEE Trans. Geosci. Remote Sens.*, submitted for publication.

874 [40] J. Sabatier, A. Fouilloux, and P. de Rosnay, "Technical implementation
875 of SMOS data in the ECMWF integrated forecast system," *IEEE Geosci.*
876 *Remote Sens. Lett.*, vol. 9, no. 2, pp. 252–256, Mar. 2012.

877 [41] [Online]. Available: <ftp://n4ftl01u.ecs.nasa.gov/SAN/AMSA/>

878 [42] C. Gruhier, P. de Rosnay, Y. Kerr, E. Ceschia, J. Calvet, and
879 P. Richaume, "Evaluation of AMSR-E soil moisture product based on
880 ground measurements over temperate and semi-arid regions," *Geophys.*
881 *Res. Lett.*, vol. 35, no. 10, p. L10 405, May 2008.

882 [43] C. Rudiger, J. C. Calvet, C. Gruhier, T. Holmes, R. de Jeu, and
883 W. Wagner, "An intercomparison of ERS-SCAT and AMSR-E soil mois-
884 ture observations with model simulations over France," *Amer. Meteorol.*
885 *Soc.*, vol. 10, no. 2, pp. 431–447, Apr. 2009.

886 [44] C. Draper, J. Walker, P. Steinle, R. de Jeu, and T. Holmes, "An evaluation
887 of AMSR-E derived soil moisture over Australia," *Remote Sens. Environ.*,
888 vol. 113, no. 4, pp. 703–710, Apr. 2009.

889 [45] C. Gruhier, P. de Rosnay, S. Hasenauer, T. Holmes, R. de Jeu, Y. Kerr,
890 E. Mougou, E. Njoku, F. Timouk, W. Wagner, and M. Zribi, "Soil moisture
891 active and passive microwave products: Intercomparison and evaluation
892 over a Sahelian site," *Hydrol. Earth Syst. Sci.*, vol. 14, no. 1, pp. 141–156,
893 Jan. 2010.

894 [46] S. Chaurasia, D. Tung, P. Thapliyal, and P. Joshi, "Assessment of AMSR-
895 E soil moisture product over India," *Int. J. Remote Sens.*, vol. 32, no. 23,
896 pp. 7955–7970, Dec. 2011.

897 [47] T. Jackson, M. Cosh, R. Bindlish, P. Starks, D. Bosch, M. Seyfried,
898 D. Goodrich, M. Moran, and J. Du, "Validation of advanced microwave
899 scanning radiometer soil moisture products," *IEEE Trans. Geosci. Remote*
900 *Sens.*, vol. 48, no. 12, pp. 4256–4272, Dec. 2010.

901 [48] B. Schweizer and E. Wolff, "On nonparametric measures of dependence
902 for random variables," *Ann. Stat.*, vol. 9, no. 4, pp. 879–885, Jul. 1981.

903 [49] Y. Wang and H. Pham, "Modeling the dependent competing risks with
904 multiple degradation processes and random shock using time-varying
905 copulas," *IEEE Trans. Rel.*, vol. 61, no. 1, pp. 13–22, Mar. 2012.

[50] C. Genest and L.-P. Rivest, "Statistical inference procedures for bivariate
906 Archimedean copulas," *J. Amer. Stat. Assoc.*, vol. 88, no. 423, pp. 1034–
907 1043, Sep. 1993.

[51] J. Fermanian, "Goodness of fit tests for copulas," *J. Multivariate Anal.*,
909 vol. 95, no. 1, pp. 119–152, Jul. 2005.

[52] C. Genest, J.-F. Quessy, and B. Rémillard, "Goodness-of-fit procedures
911 for copula models based on the probability integral transform," *Scand. J.*
912 *Stat.*, vol. 33, no. 2, pp. 337–366, Jun. 2006.

[53] C. Genest and B. Rémillard, "Validity of the parametric bootstrap
914 for goodness-of-fit testing in semiparametric models," *Annales Henri*
915 *Poincaré*, vol. 44, no. 6, pp. 1096–1127, 2008.

[54] D. Berg, "Copula goodness-of-fit testing: An overview and power com-
917 parison," *Eur. J. Finance*, vol. 15, no. 7/8, pp. 675–701, 2009.

[55] C. Genest, B. Rémillard, and D. Beaudoin, "Goodness-of-fit tests for
919 copulas: A review and a power study," *Insurance: Math. Econom.*, vol. 44,
920 no. 2, pp. 199–213, Apr. 2009.

[56] D. Huard, G. Evin, and A. Favre, "Bayesian copula selection," *Comput.*
922 *Stat. Data Anal.*, vol. 51, no. 2, pp. 809–822, Nov. 2006.



Delphine J. Leroux received the M.S. degree in 924
applied mathematics from Institut National des Sci- 925
ences Appliquées, Toulouse, France, in 2009 and the 926
Ph.D. degree in spatial hydrology from Université 927
Paul Sabatier, Toulouse, in 2012. 928

From 2009 to 2012, she was with the Centre 929
d'Etudes Spatiales de la Biosphère, Toulouse, where 930
she worked on the validation of the Soil Moisture 931
and Ocean Salinity soil moisture product at the local 932
and global scales by using statistical and physical 933
methods. She is currently with the Jet Propulsion 934

Laboratory (JPL), Pasadena, CA, USA, on the Soil Moisture Active Passive 935
mission. 936

AQ28



Yann H. Kerr (M'88–SM'01–F'13) received the 937
engineering degree from Ecole Nationale Supérieure 938
de l'Aéronautique et de l'Espace, Toulouse, France, 939
the M.Sc. degree in electronics and electrical engi- 940
neering from Glasgow University, Glasgow, U.K., 941
and the Ph.D. degree in astrophysique géophysique 942
et techniques spatiales from Université Paul Sabatier, 943
Toulouse. 944

He is currently the Director of the Centre d'Etudes 945
Spatiales de la Biosphère, Toulouse. His fields of 946
interest are in the theory and techniques for mi- 947

948
949
950
951
952
953
954
955
956
957
958
959
960
961
962

crowave and thermal infrared remote sensing of the Earth, with emphasis
on hydrology and water resource management. He was an EOS Principal
Investigator (interdisciplinary investigations) and PI and precursor of the use
of the SCAT over land. In 1990, he started to work on the interferometric
concept applied to passive microwave Earth observation and was subsequently
the Science Lead on the MIRAS project for ESA. In 1997, he proposed the
Soil Moisture and Ocean Salinity (SMOS) mission, the natural outcome of the
previous MIRAS work. He is currently involved in the exploitation of SMOS
data, in the Cal Val activities and related level 2 soil moisture and level 3 and 4
developments. He is also working on the SMOS next concept.

Dr. Kerr received the World Meteorological Organization 1st prize (Norbert
Gerber), the USDA Secretary's team award for excellence (Salsa Program),
and the GRSS certificate of recognition for leadership in the development of
the first synthetic aperture microwave radiometer in space and success of the
SMOS mission and is a Distinguished Lecturer for GRSS.

AQ29

AQ30

AQ31

AQ32

AQ33

AQ34

AQ35

AQ36

AQ37

AQ38

AQ39

AQ27



Eric F. Wood received the B.A.Sc. degree in civil engineering from the University of British Columbia, Vancouver, BC, Canada, in 1970 and the S.M., C.E., and Sc.D. degrees in civil engineering from the Massachusetts Institute of Technology, Cambridge, MA, USA, in 1972, 1973, and 1974, respectively.

He is currently a Professor in the Department of Civil and Environmental Engineering, Princeton University, NJ, USA. His recent contributions include the macroscale hydrologic prediction of the coupled water and energy balances of the land surface, remote sensing as an integral tool for observation and modeling of the hydrologic cycle, and developing and evaluating seasonal hydrological forecasts based on coupled seasonal climate forecasts.

Dr. Wood is a fellow of the American Geophysical Union and the American Meteorological Society. He received, among other honors, the Robert E. Horton Award from the Hydrology Section of the American Geophysical Union (1977), the John Dalton Medal from the European Geophysical Union (2007), and the Jules G. Charney Award from the American Meteorological Society (2010).



Alok K. Sahoo received the Ph.D. degree in computational sciences from George Mason University, Fairfax, VA, USA, in 2008.

After finishing his Ph.D., he worked as a Research Associate at the Institute of Global Environment and Society, Beltsville, MD, USA, from 2008 to 2009. He is currently an Associate Research Hydrologist with the Department of Civil and Environmental Engineering, Princeton University, Princeton, NJ, USA. His research interests involve the application of microwave remote sensing in hydrologic applications.

His current research projects include soil moisture estimation from microwave sensors and checking consistency among hydrologic cycle variables for drought monitoring.



Rajat Bindlish (S'98-AM'99-M'03-SM'05) received the B.S. degree in civil engineering from the Indian Institute of Technology, Bombay in 1993 and the M.S. and Ph.D. degrees in civil engineering from The Pennsylvania State University in 1996 and 2000, respectively.

He is currently with SSAI, working at USDA Agricultural Research Service, Hydrology and Remote Sensing Laboratory, Beltsville, MD, USA. His research interests involve the application of microwave remote sensing in hydrology. He is currently working on soil moisture estimation from microwave sensors and their subsequent application in land surface hydrology.



Thomas J. Jackson (SM'96-F'02) received the Ph.D. degree from the University of Maryland, College Park, MD, USA, in 1976.

He is a Research Hydrologist with the U.S. Department of Agriculture, Agricultural Research Service, Hydrology and Remote Sensing Laboratory, Beltsville, MD, USA. His research involves the application and development of remote sensing technology in hydrology and agriculture, primarily the microwave measurement of soil moisture.

Dr. Jackson is or has been a member of the science and validation teams of the Aqua, ADEOS-II, Radarsat, Oceansat-1, Envisat, ALOS, Soil Moisture and Ocean Salinity, Aquarius, GCOM-W, and Soil Moisture Active Passive remote sensing satellites. He is a fellow of the Society of Photo-Optical Instrumentation Engineers, the American Meteorological Society, and the American Geophysical Union. In 2003, he received the William T. Pecora Award (NASA and Department of Interior) for outstanding contributions toward understanding the Earth by means of remote sensing and the AGU Hydrologic Sciences Award for outstanding contributions to the science of hydrology. He received the IEEE Geoscience and Remote Sensing Society Distinguished Achievement Award in 2011.

AUTHOR QUERIES

AUTHOR PLEASE ANSWER ALL QUERIES

Please be aware that the authors are required to pay overlength page charges (\$200 per page) if the paper is longer than 6 pages. If you cannot pay any or all of these charges please let us know.

This pdf contains 2 proofs. The first half is the version that will appear on Xplore. The second half is the version that will appear in print. If you have any figures to print in color, they will be in color in both proofs.

- AQ1 = The sentence was restructured for clarity. Please check if the original thought was retained, and correct if necessary.
- AQ2 = Please provide the expanded form of “USDA.”
- AQ3 = Please provide the expanded form of “ARS.”
- AQ4 = The sentence was restructured for clarity. Please check if the original thought was retained, and correct if necessary.
- AQ5 = The sentence was restructured for clarity. Please check if the original thought was retained, and correct if necessary.
- AQ6 = “AMSR-E” is defined as “Advanced Microwave Scanning Radiometer-Earth Observing System” for consistency. Please check if appropriate, and correct if necessary.
- AQ7 = The sentence was restructured for clarity. Please check if the original thought was retained, and correct if necessary.
- AQ8 = “Picard *et al.*” was changed to “Picard and Fily.” Please check if appropriate, and correct if necessary.”
- AQ9 = The sentence was rephrased for clarity. Please check if the original thought was retained, and correct if necessary.
- AQ10 = The sentence was rephrased for clarity. Please check if the original thought was retained, and correct if necessary.
- AQ11 = The sentence was rephrased for clarity. Please check if the original thought was retained, and correct if necessary.
- AQ12 = The sentence was restructured for clarity. Please check if the original thought was retained, and correct if necessary.
- AQ13 = “rmse” is defined as “root-mean-square error.” Please check if appropriate, and correct if necessary.”
- AQ14 = The sentence was rephrased. Please check if the original thought was retained, and correct if necessary.”
- AQ15 = Please provide the expanded form of “NASA.”
- AQ16 = The sentence was rephrased for clarity. Please check if the original thought was retained, and correct if necessary.
- AQ17 = The sentence was rephrased for clarity. Please check if the original thought was retained, and correct if necessary.
- AQ18 = The caption was rephrased for clarity. Please check if the original thought was retained, and correct if necessary.
- AQ19 = The sentence was rephrased for clarity. Please check if the original thought was retained, and correct if necessary.
- AQ20 = “CDF” is defined as “cumulative density function” for consistency. Please check if appropriate, and correct if necessary.
- AQ21 = The sentence was rephrased for clarity. Please check if the original thought was retained, and correct if necessary.

- AQ22 = The sentence was rephrased for clarity. Please check if the original thought was retained, and correct if necessary.
- AQ23 = The sentence was rephrased for clarity. Please check if the original thought was retained, and correct if necessary.
- AQ24 = The sentence was rephrased for clarity. Please check if the original thought was retained, and correct if necessary.
- AQ25 = The sentence was rephrased for clarity. Please check if the original thought was retained, and correct if necessary.
- AQ26 = The sentence was rephrased for clarity. Please check if the original thought was retained, and correct if necessary.
- AQ27 = Please provide publication update in Ref. [39].
- AQ28 = The author's current affiliation indicated in the footnote did not correspond to the current affiliation provided in the curriculum vitae. Please check.
- AQ29 = The sentence was rephrased for clarity. Please check if the original thought was retained, and correct if necessary.
- AQ30 = The sentence was rephrased for clarity. Please check if the original thought was retained, and correct if necessary.
- AQ31 = Please provide the expanded form of "EOS."
- AQ32 = Please provide the expanded form of "PI."
- AQ33 = Please provide the expanded form of "SCAT."
- AQ34 = Please provide the expanded form of "MIRAS."
- AQ35 = Please provide the expanded form of "ESA."
- AQ36 = Please provide the expanded form of "Cal Val."
- AQ37 = "Dr." was inserted as the title for author Yann H. Kerr. Please check if appropriate, and correct if necessary.
- AQ38 = Please provide the expanded form of "GRSS."
- AQ39 = The sentence was rephrased for clarity. Please check if the original thought was retained, and correct if necessary.
- AQ40 = Please provide the specific location of the Indian Institute of Technology, Bombay.
- AQ41 = Please provide the specific location of The Pennsylvania State University.
- AQ42 = Please provide the expanded form of "SSAI."
- AQ43 = Please provide the expanded form of "ADEOS-II."
- AQ44 = Please provide the expanded form of "ALOS."
- AQ45 = Please provide the expanded form of "GCOM-W."
- AQ46 = Please provide the expanded form of "AGU."

END OF ALL QUERIES